JOURNAL OF VIROLOGY, Sept. 2003, p. 9346–9358 Vol. 77, No. 17
0022-538X/03/$08.00+0 DOI: 10.1128/JVI.77.17.9346–9358.2003

Activation of Mitogen-Activated Protein Kinase and NF-κB Pathways by a Kaposi's Sarcoma-Associated Herpesvirus K15 Membrane Protein

Melanie M. Brinkmann,[1] Mark Glenn,[1]† Lucille Rainbow,[2] Arnd Kieser,[3] Cornelia Henke-Gendo,[1] and Thomas F. Schulz[1]*

Institut für Virologie, Medizinische Hochschule Hannover, D-30625 Hannover,[1] and GSF-National Research Center for Environment and Health, Institute for Clinical Molecular Biology and Tumor Genetics, D-81377 Munich,[3] Germany, and Department of Medical Microbiology, The University of Liverpool, Liverpool, United Kingdom[2]

Received 27 February 2003/Accepted 10 June 2003

The K15 gene of Kaposi's sarcoma-associated herpesvirus (also known as human herpesvirus 8) consists of eight alternatively spliced exons and has been predicted to encode membrane proteins with a variable number of transmembrane regions and a common C-terminal cytoplasmic domain with putative binding sites for SH2 and SH3 domains, as well as for tumor necrosis factor receptor-associated factors. These features are reminiscent of the latent membrane proteins LMP-1 and LMP2A of Epstein-Barr virus and, more distantly, of the STP, Tip, and Tio proteins of the related γ_2-herpesviruses herpesvirus saimiri and herpesvirus ateles. These viral membrane proteins can activate a number of intracellular signaling pathways. We have therefore examined the abilities of different K15-encoded proteins to initiate intracellular signaling. We found that a 45-kDa K15 protein derived from all eight K15 exons and containing 12 predicted transmembrane domains in addition to the cytoplasmic domain activated the Ras/mitogen-activated protein kinase (MAPK) and NF-κB pathways, as well as (more weakly) the c-Jun N-terminal kinase/SAPK pathway. Activation of the MAPK and NF-κB pathways required phosphorylation of tyrosine residue 481 within a putative SH2-binding site (YEEVL). This motif was phosphorylated by the tyrosine kinases Src, Lck, Yes, Hck, and Fyn. The region containing the YEEVL motif interacted with tumor necrosis factor receptor-associated factor 2 (TRAF-2), and a dominant negative TRAF-2 mutant inhibited the K15-mediated activation of the Ras/MAPK pathway, suggesting the involvement of TRAF-2 in the initiation of these signaling routes. In contrast, several smaller K15 protein isoforms activated these pathways only weakly. All of the K15 isoforms tested were, however, localized in lipid rafts, suggesting that incorporation into lipid rafts is not sufficient to initiate signaling. Additional regions of K15, located presumably in exons 2 to 5, may therefore contribute to the activation of these pathways. These findings illustrate that the 45-kDa K15 protein engages pathways similar to LMP1, LMP2A, STP, Tip, and Tio but combines functional features that are separated between LMP1 and LMP2A or STP and Tip.

Kaposi's sarcoma (KS)-associated herpesvirus (KSHV) or human herpesvirus 8 (13) is a human type 2 gammaherpesvirus found in all forms of KS (57, 72), in primary effusion lymphoma (PEL) (12), and in the plasma cell variant of multicentric Castleman's disease (76). Strong epidemiological evidence suggests that KSHV plays an indispensable role in the pathogenesis of KS but that additional factors, such as immune suppression or coinfection with HIV, are required for the manifestation of this tumor (72, 73). KSHV is present in the endothelial and spindle (tumor) cells of KS lesions, in PEL cells, and in perifollicular B cells of multicentric Castleman's disease, where it persists in a latent form with limited viral gene expression (6, 22, 43, 62, 65). In these tumor cells, lytic viral replication occurs in a subpopulation of KSHV-infected cells (5, 16, 43, 62).

The K15 gene of KSHV is located adjacent to the terminal repeat region at the right end of the KSHV long unique coding region and consists of eight differentially spliced exons (17, 34, 64). The sequences of all of the K15 cDNA clones isolated so far (17, 34; M. M. Brinkmann et al., unpublished data) are predicted to contain a common C-terminal cytoplasmic region linked to a variable number of transmembrane domains (Fig. 1). The cytoplasmic region (amino acids [aa] 355 to 489) contains one putative SH2-binding site motif, Y^{481}EEVL, a second tyrosine-containing motif (Y^{431}ASIL) of the general Yxxθ consensus found in SH2-binding sites and cytoplasmic internalization motifs, a putative proline-rich SH3-binding site, and a putative TRAF-binding site (A^{473}TQPTDD) (17, 34, 64). These sequence motifs are conserved between the two highly divergent M and P genotypes of KSHV that have been found in this region of the KSHV genome, suggesting the conservation of associated functional properties (34, 64). Phosphorylation of Y^{481} in the YEEVL motif (17) and binding of TRAF-1, -2, and -3 to the cytoplasmic domain of K15 (34) have been observed.

* Corresponding author. Mailing address: Institut für Virologie, Medizinische Hochschule Hannover, Carl-Neuberg Strasse 1, 30625 Hannover, Germany. Phone: 49-511-532-6736. Fax: 49-511-532-8736. E-mail: tschulz@virologie.mh-hannover.de.

† Present address: Department of Haematology, The University of Liverpool, Liverpool, United Kingdom.

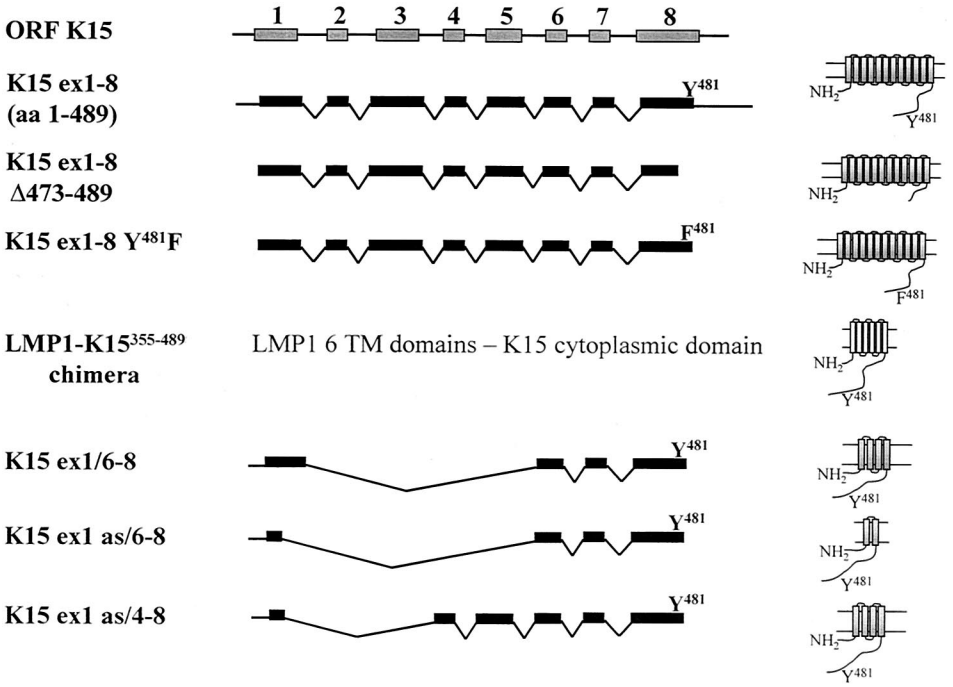

FIG. 1. ORF K15 expression constructs used in this study and their putative protein products. The K15 ORF is multiply and alternatively spliced (as). The major transcript identified in PEL cells by RT-PCR is fully spliced and contains all eight exons (K15 ex1-8; aa 1 to 489). It encodes a membrane protein with up to 12 transmembrane domains and a cytoplasmic C-terminal domain (aa 355 to 489). The C-terminal domain contains motifs reminiscent of SH2, SH3, and TRAF-like binding sites. The distal TRAF-like binding site and the distal SH2-binding motif Y^{481}EEVL are deleted in construct K15 ex1-8 Δ473 to 489. K15 ex1-8 Y^{481}F carries a point mutation in the distal SH2-binding motif ($Y^{481\rightarrow}F^{481}$EEVL). The LMP1–$K15^{355\text{-}489}$ chimera was constructed by fusing the six transmembrane domains of LMP1 to the cytoplasmic C-terminal end (aa 355 to 489) of K15. The splice variants K15 ex1/6-8, K15 ex1 as/6-8, and K15 ex1 as/4-8 differ in the number of transmembrane domains they contain, but all contain the C-terminal domain.

The combination of multiple transmembrane regions with a cytoplasmic domain that can be phosphorylated on tyrosines and/or interact with TRAFs is reminiscent of the latent membrane proteins LMP1 and LMP2A of Epstein-Barr virus (EBV). LMP1 and LMP2A are both located at the ends of the coding region of the EBV genome, with LMP2A located in the position corresponding to that of K15, while LMP1 occupies the position corresponding to that of another KSHV membrane protein, K1. K1 has transforming properties (48) and triggers a number of intracellular signaling pathways (49). LMP1 is considered to be essential for the tumorigenic properties of EBV by virtue of its ability to activate the pathways for NF-κB, c-Jun N-terminal kinase (JNK)/SAPK, p38 MAPK, and JAK/STAT (reviewed in reference 47). Activation of these signaling pathways requires the multimerization of LMP-1 molecules in the membrane through its six membrane-spanning domains and the interaction of cellular signaling components with different regions in its cytoplasmic domain (47). Among these, so-called C-terminal activator region 1 (CTAR-1) interacts with TRAF-1, -2, -3, and -5 and activates the NF-κB pathway, while the more distal region CTAR-2 associates directly with TRADD and indirectly with TRAF-2 and initiates the cascades leading to the activation of JNK/SAPK and NF-κB (8, 19, 20, 37, 40, 44, 45, 46, 56, 58, 68). The region between CTAR-1 and -2 has been reported to be involved in triggering of the JAK/STAT cascade (33).

LMP2A consists of an N-terminal cytoplasmic domain of 119 aa and a membrane anchor region of 12 transmembrane segments. The cytoplasmic domain contains several SH2-binding sites surrounding tyrosine residues, of which two, Y74 and Y85, are grouped as an ITAM (immune receptor tyrosine-based activation motif) (reviewed in reference 51). Tyrosine 112 is part of a YEEA motif that resembles the YEEI/L consensus sequence for Src SH2-binding domains. LMP2A is expressed in latently EBV-infected circulating B cells and in B-lymphoma cells of large-cell lymphoma in immunocompromised individuals or those with Hodgkin's disease (reviewed in reference 66). In B cells, binding of the Src kinase Lyn to the YEEA motif leads to phosphorylation of the ITAM, which in turn leads to recruitment of the tyrosine kinase Syk (50, 61). This sequence of events is similar to the early signaling steps that occur after triggering of the B- or T-cell receptor: here, the initial phosphorylation of the ITAM in cytoplasmic components of the receptor complex leads to the recruitment of Syk (in B cells) or Zap70 (in T cells) and binding of the tandem SH2 domains in the recruited kinases to the two phosphorylated tyrosine residues in the ITAM. The interactions of LMP2A with the components of these signaling cascades lead to inhibition of B-cell receptor signaling (29, 30, 54). LMP2A interacts with the WW domain containing ubiquitin ligases Nedd4, WWP2/AIP2, and AIP4 via a PPPPY motif and thereby induces the ubiquitination and rapid proteasome-mediated turnover of the LMP2A-associated protein tyrosine kinases (PTKs) (38, 39, 78). It is thought that this contributes to

the survival of EBV in infected B cells, since the effect of LMP2A would be to inhibit the activation of infected B cells by antigen and with it the activation of the viral lytic cycle (51). However, transgenic expression of LMP2A in murine B cells increases B-cell survival (10, 11, 51, 53) and therefore LMP2A may also make a more direct contribution to the survival of EBV-infected B cells. Unlike its counterpart LMP1, however, LMP2A is not required for the immortalization of EBV-infected B cells.

LMP2A is also expressed in the tumor-derived epithelial cells of nasopharyngeal carcinoma (reviewed in reference 66). Experimental expression of LMP2A in epithelial cells leads to the acquisition of phenotypic characteristics of transformation such as growth in soft agar and dedifferentiation and the activation by LMP2A of the phosphatidylinositol 3 kinase/Akt pathway is important for this LMP2A-induced phenotype (70). In epithelial cells, LMP2A phosphorylation can be triggered by adherence of these cells to extracellular matrix proteins and involves the regulator of Src, the C-terminal Src kinase Csk (69). LMP2A also binds to and is phosphorylated by the mitogen-activated protein kinase (MAPK) ERK1 (61). A recent report found that LMP2A activates the MAPKs Erk and JNK in B cells (15), but others have not observed Erk activation by LMP2A in epithelial cells (70).

Similar to the EBV LMPs, at least two New World primate γ_2-herpesviruses, herpesvirus saimiri (HVS) and herpesvirus ateles (HVA), also encode membrane-associated proteins, STP, Tip (HVS), and Tio (HVA), that can either bind to TRAFs (STP) or are phosphorylated by members of the Src kinase family (Tip, Tio) (1; reviewed in reference 18). STP of HVS strains A and C is required for the transforming and/or lymphomagenic potential of these viruses (reviewed in reference 18). HVS and HVA are T lymphotropic, and HVS strain C Tip is phosphorylated by the Src kinase Lck and can inhibit T-cell receptor-induced signaling (4, 41). Tip may also have a modulatory role in STP-mediated transformation (18, 21).

Given the presumed roles of LMP1, LMP2A, STP, Tip, and Tio in immortalization, dedifferentiation, maintenance of latency, and regulation of the viral lytic replication cycle, we wanted to investigate whether KSHV K15-derived proteins have similar functions. As a first step, we sought to identify cellular signaling pathways triggered by K15 proteins and show here that the longest K15 isoform, but not the smaller isoforms, activate the Ras/MAPK and NF-κB pathways following phosphorylation of a tyrosine residue in a YEEVL motif by several members of the Src kinase family.

MATERIALS AND METHODS

Cell culture methods, transfections, and MEK1/2 inhibitors. The cell lines HEK (human embryonic kidney) 293-T, HEK 293, and Cos7 were cultured in Dulbecco's modified Eagle's medium (Gibco) supplemented with 10% heat-inactivated fetal calf serum (FCS), 50 IU of penicillin per ml, 50 μg of streptomycin per ml, and 300 μg of L-glutamine per ml at 37°C in humidified air with 5% CO_2. For transfections, cells were grown to subconfluence in six-well plates (Greiner). HEK 293-T and 293 cells were transfected with FuGENE transfection reagent (Roche; FuGENE-to-DNA ratio of 3 μl to 1 μg), Cos7 cells were transfected with the Effectene transfection reagent (Qiagen) in accordance with the manufacturer's instructions. Total amounts of transfected DNA were adjusted with salmon testis DNA (Sigma). The specific MEK1/2 inhibitors PD98059 and UO126 (Calbiochem) were used at a concentration of 50 μM from a 50 mM stock solution in dimethyl sulfoxide (DMSO). The inhibitors were added to the medium 14 h after transfection, and cells were incubated for a further 8 h before being extracted as described below.

DNA constructs. The full-length K15 cDNA clone (K15 aa 1 to 489) from the BCP-1 KSHV isolate (primary effusion cell line infected with KSHV; 7) was generated by reverse transcription (RT)-PCR amplification of the K15 region with the forward primer LRH6for, which binds 192 bp upstream of the putative start codon of K15 (5′-ATCCGGAATATTTATGAGCC-3′), and primer ex8arev, which binds to the start region of open reading frame 75 (ORF75) 245 nucleotides downstream of the K15 stop codon (5′-CTCCAACCACAGCCCA GTGACG-3′). The resulting PCR product was cloned into pGEM-T (Promega) and sequenced. The PCR product was then cloned into the eucaryotic expression vector pFJEA by digestion with *Eco*RI (clone MBK15). Clone 35, which contains a full-length cDNA (exons 1 to 8) of K15 from the BCBL-1 PEL cell line cloned into the *Eco*RI/*Xba*I sites of pFJEA was kindly provided by J.-K. Choi (17). Clone 35 contains an artificial Kozak sequence, begins at the putative start codon of K15 in exon 1, and contains a Flag tag at its C-terminal end. Plasmid K15 ex1-8 (aa Δ473 to 489) lacking the C-terminal 17 aa and plasmid K15 ex1-8 $Y^{481}F$ carrying the Y481→F point mutation in the Y^{481}EEVL motif were generated by PCR amplification of clone 35 with the upstream primer LAMPB5′ (5′-ACAG GATCCTAAAATGAAGACACTCATATTCTTCTGG-3′) and the reverse primer ex8ad1 (5′-ACGCCCGGGTTAGGCTTGGGCGGTGTCTATACGGA AGGC-3′) or ex8aY:F (5′-TATGAATTCCTAGTTCCTGGGAAATAAAACC TCCTCAAACAGGTC-3′), respectively. PCR products were cloned into pGEM-T and subsequently cloned into the *Not*I site of pFJEA and sequenced.

The cDNAs of the K15 splice variants K15 ex1/6-8, K15 ex1 as/6-8, and K15 ex1 as/4-8 were generated by RT-PCR amplification of the K15 region (BCP-1 KSHV isolate) with primers LR65 (5′-ACGATCTAGATCCGGAATATTTAT GAGC-3′) and ex8arev, followed by a nested PCR with forward primer FJLampfor (5′-ATCGAATTCCATTTACAACAACTCTATTG-3′), binding 45 nucleotides upstream of the K15 start codon, and reverse primer FJLamprev (5′-ATC GGTACCTAGTTCCTGGGAAATAAAAC-3′), binding at the K15 stop codon. PCR products were cloned into pGEM-T, sequenced, and subsequently cloned into the *Eco*RI and *Kpn*I sites of pFJEA.

A plasmid containing the entire predicted cytoplasmic domain (aa 355 to 489) of K15 fused to glutathione *S*-transferase (GST) (pGEX8A, GST–$K15^{355\text{-}489}$) has been previously described (34). A further GST fusion plasmid in which the carboxy-terminal 17 aa of K15 were deleted (GST–$K15^{355\text{-}472}$) was generated by PCR with the 5′ primer GSTex8afor (5′-CAGGGATCCTAAATAGTTACCG ACAGAGAAGGGG-3′) and the 3′ primer ex8arevd1. Further deletion constructs of the K15 C-terminal region of the GST-K15 fusion protein were generated with plasmid pGEX8A (GST–$K15^{355\text{-}489}$) as the template together with primer GSTex8afor and either reverse primer ex8arevd2 (5′-ACTCCCGGGAC CGGACACTAAAATACTGGC-3′) to generate GST–$K15^{355\text{-}438}$ or reverse primer ex8arevd4 (5′-ACTCCCGGGTGTGGTGTAAGTTCTGGTCCC-3′) to generate GST–$K15^{355\text{-}373}$. PCR products were cloned into pGEX-3X (Amersham Pharmacia) and sequenced.

The LMP1–$K15^{355\text{-}489}$ chimera, consisting of the six amino-terminal transmembrane domains of LMP1 and the cytoplasmic region of K15, was constructed by amplification of the transmembrane domain of LMP1 from plasmid pSG5-LMP1 (37) with primers LMPLAMPa5′ (5′-GACGGTACCATGGACTACAA GGACGATGACGACAAGGAACAC GACCTTGAGAGGGGCCCACCG-3′) and LMPLAMPa3′ (5′-CCTTCTCTGTCGGTAACTATTTACTTCATCAC TGTGTCGTTGTCCATGG-3′). Primer LMPLAMPa5′ introduces the Flag epitope tag DYKDDDDK (sequence underlined), while the first 25 nucleotides of LMPLAMPa3′ are homologous to a region within the carboxy terminus of K15 (sequence underlined). The resulting amplicon was purified and used as a primer together with primer LAMPa3′ (5′-TATGAATTCCTAGTTCCTGGG AAATAAAAC-3′) in a PCR with genomic BCP-1 DNA as the template. The resulting product was cloned into pcDNA3.1 (Invitrogen) and sequenced.

cDNA plasmids expressing Flag-tagged TRAF-1, -2, and -3 were kindly provided by M. Rothe. Myc-tagged PTK expression plasmids for Src, Fyn, Hck, Lck, and Yes were kindly provided by S. Müller, Erlangen, Germany. pSRα-HA-JNK1 and pSRα-HA-Erk2 (55); pCMV-HA-p38 (3); the AP-1 reporter constructs pRTU14 (luciferase reporter gene under the control of a minimal promoter and four TREs [TPA response elements]) and pRTU1 (lacking the TREs) (45); GST–c-Jun (45); dominant negative mutant forms of TRAF-2 (pRK-TRAF-2 [aa 87 to 501]) (36, 59), TRAF-6 (aa 300 to 524) (71), and Ras (N-17); expression vectors pCis2 and pRKH5; and the construct pSV-LMP1 (45) have been described previously. Dominant negative Erk2 C3 (Y185→F) (52, 67, 77), RSV Raf C4B (9, 28), and eucaryotic expression vector KRSPA (Rous sarcoma virus promoter) were kind gifts from S. Ludwig. The NF-κB reporter plasmid p3EnhκBconA-Luc containing three NF-κB sites upstream of the firefly luciferase gene (23) and pSG5-LMP1 were provided by A. Eliopoulos.

Expression and purification of recombinant proteins and GST fusion protein binding assays. GST–c-Jun, GST–K15$^{355\text{-}489}$, and GST–K15$^{355\text{-}472}$ for radioactive immunocomplex kinase assays were purified as described in reference 45. The purified GST fusion proteins eluted with glutathione were analyzed by sodium dodecyl sulfate (SDS)-polyacrylamide gel electrophoresis (PAGE).

For GST pulldown experiments, *Escherichia coli* M15 cultures transformed with the GST-K15 expression plasmids or GST alone were grown at 37°C in 2YT medium plus ampicillin, induced at an optical density at 600 nm of 0.2 to 0.3 with 1 mM isopropyl-β-D-thiogalactopyranoside (IPTG), and harvested by centrifugation 6 h after induction. The pellet was resuspended in 1,000 μl of phosphate-buffered saline (PBS) plus protease inhibitors per 10 ml of culture to an optical density at 600 nm of 2.5. After sonication on ice, Triton X-100 was added to a 1% final concentration, and the cells were kept on ice for 10 min and then centrifuged for 15 min at 14,000 × *g* at 4°C. The supernatant was adsorbed onto 20 to 50 μl of glutathione Sepharose beads for 1 h at 4°C, after which the beads were washed twice in PBS and then once in 1% NP-40 lysis buffer (50 mM Tris-HCl [pH 7.4], 150 mM NaCl, 1 mM EDTA, 1% NP-40). HEK 293 or 293-T cells were transfected as mentioned in the section on coimmunoprecipitation but with 1 μg of cDNA expression constructs per well of a six-well plate of either Flag-tagged TRAF-1, -2, or -3 (HEK 293) or the myc-tagged Src kinase Src, Lck, Yes, Fyn, or Hck (HEK 293-T). At 48 h after transfection, cells were washed once on ice with PBS and lysed in 1% NP-40 lysis buffer containing protease inhibitors for 10 min on ice. Cell lysates were centrifuged at 14,000 × *g* for 10 min at 4°C and precleared by incubation with 50 μl of glutathione beads for 1 h at 4°C. Cleared lysates were then incubated for 1 h or overnight at 4°C with either GST control protein or GST-K15 fusion protein immobilized to glutathione beads. The beads were washed three times in 1% NP-40 lysis buffer, and proteins adsorbed to beads were boiled in 50 μl of SDS electrophoresis sample buffer and analyzed by SDS-PAGE and Western blotting.

Generation of rabbit polyclonal and mouse monoclonal antibodies to the C-terminal K15 domain. The carboxy-terminal region of K15 was transferred from plasmid pGEX8A to plasmid pGEX6A. The GST–K15$^{355\text{-}489}$ fusion protein was prepared from 1-liter *E. coli* (M15) cultures, and the K15 portion of the protein was cleaved by incubation in the presence of PreScission protease while still bound to GST beads in accordance with the manufacturer's (Amersham Pharmacia) instructions. The cleaved C-terminal cytoplasmic domain of K15 (aa 355 to 489) was eluted with PBS and used to immunize two rabbits in accordance with standard protocols. Noncleaved GST–K15$^{355\text{-}489}$ fusion protein was used to immunize mice in accordance with standard protocols.

Immunocomplex kinase assays and Western blotting (immunoblotting). As indicated in the figure legends, HEK 293-T cells were cotransfected with 1 μg of hemagglutinin (HA)-tagged MAPK and 1 μg of K15 cDNA expression constructs with FuGENE. Where indicated, 700 ng of dominant negative mutants or their respective empty expression vectors were also cotransfected. After transfection, cells were maintained in medium containing 1% FCS to downregulate serum-activated signaling pathways. At 24 h after transfection, cells were lysed in TBS-T buffer (20 mM Tris-HCl [pH 7.4], 150 mM NaCl, 1 mM EDTA, 1% Triton X-100; the protease inhibitors phenylmethylsulfonyl fluoride [PMSF; 1 mM], leupeptin [50 μM], aprotinin [100 U/ml], benzamidine [200 μM], and pepstatin A [1 μM]; and the phosphatase inhibitors sodium orthovanadate, β-glycerophosphate, sodium molybdate, sodium fluoride, sodium pyrophosphate at 0.5 mM). Cleared lysates were incubated overnight with anti-HA monoclonal antibody 12CA5 (Boehringer Mannheim) immobilized to protein G Sepharose beads (Amersham Pharmacia) to immunoprecipitate HA-tagged kinases. Afterwards, samples were centrifuged and the supernatants were analyzed for expression of K15 constructs by Western blotting. Beads with bound MAPK were washed twice with TBS-T and twice with kinase reaction buffer (20 mM Tris-HCl [pH 7.4], 20 mM NaCl, 1 mM dithiothreitol, 10 mM $MgCl_2$, 2 μM ATP, 0.5 mM β-glycerophosphate, 0.5 mM sodium orthovanadate). In vitro kinase reactions to assay the activity of immunoprecipitated HA-MAPK were performed in kinase reaction buffer in the presence of 10 μCi of [γ-^{32}P]ATP (10 mCi/ml; Hartmann Analytics) per reaction sample with 200 ng of bovine myelin basic protein (MBP; Sigma), ATF2 fusion protein (34 kDa; Cell Signaling), or purified GST–c-Jun as a substrate. Kinase reactions were stopped after 30 min at 25°C with electrophoresis sample buffer, and the reaction mixtures were heated for 5 min at 100°C, separated by SDS-PAGE, blotted onto Hybond-C membranes (Amersham Pharmacia), and analyzed by autoradiography.

For the Src kinase assay, HEK 293-T cells were transfected with either 1 μg of expression plasmids for myc-tagged Src kinase Src, Hck, Lck, Yes, or Fyn or the empty expression vector. After transfection, cells were kept in complete medium with 10% FCS and cells were lysed 24 h posttransfection in TBS-T as mentioned above. Immunoprecipitation of the myc-tagged Src kinase was carried out overnight with anti-c-*myc* antibody-coated beads (Clontech). The in vitro kinase reaction was done as described above but with 200 ng of purified GST–K15$^{355\text{-}489}$ or GST–K15$^{355\text{-}472}$ fusion protein as the substrate.

For detection of proteins by Western blotting, cleared cell lysates or fractions of the sucrose gradient containing K15 proteins were not boiled prior to SDS-PAGE. As indicated, the following primary antibodies were used for immunostaining of immunoblots: rabbit anti-JNK1 C-17, mouse anti-Erk2 D-2, rabbit anti-p38 MAPK H-147, anti-caveolin 1 (all Santa Cruz Biotech), mouse anti-c-myc 9E10 (BIOMOL), mouse antiphosphotyrosine P-Thyr-100 (Cell Signaling), and mouse anti-Flag M2 (Sigma). Immunoblots were analyzed with horseradish peroxidase-coupled secondary antibodies (DAKO) and a standard enhanced-chemiluminescence reaction (Perkin-Elmer).

Coimmunoprecipitation. One day prior to transfection, 3×10^5 HEK 293 cells were plated into each well of a six-well plate. The cells were transiently transfected with 500 ng of either plasmid LMP1–K15$^{355\text{-}489}$ or the deletion mutant form LMP1–K15$^{355\text{-}472}$ and 1 μg of the cDNA expression construct for Flag-tagged TRAF-1, -2, or -3 with the FuGENE transfection reagent. At 48 h posttransfection, cells were washed once in PBS and lysed in 1% NP-40 lysis buffer containing protease inhibitors (see above). Lysates were cleared by centrifugation, and supernatants were precleared with 50 μl of protein G Sepharose (Amersham Pharmacia). To 100 μl of precleared lysate, 0.5 μl of rabbit anti-K15 serum was added. After 1 h of incubation on ice, the protein-antibody complexes were incubated with 20 μl of protein G Sepharose beads at 4°C with gentle shaking for 2 h. Beads were washed three times with 1% NP-40 lysis buffer, and bound proteins were recovered by boiling in SDS-PAGE sample buffer. Eluted proteins were analyzed by Western blotting as described above.

Luciferase-based reporter assays. To assay NF-κB activity, HEK 293-T cells were transiently cotransfected with 50 ng of the NF-κB luciferase reporter plasmid p3EnhκBconA-Luc containing three tandem repeats of the NF-κB sites from the immunoglobulin Gκ promoter and the indicated amounts of K15 expression constructs or LMP1, as mentioned in the figure legends, per well of a six-well plate. At 24 h posttransfection, cells were washed with PBS and lysed in reporter lysis buffer (Promega). Luciferase activities were measured in cleared lysates with a luciferase assay system in accordance with the manufacturer's (Promega) instructions. NF-κB activity was calculated as fold induction compared to that of mock (empty expression vector)-transfected controls.

For analysis of AP-1 activity, 50 ng of the reporter plasmid pRTU14 or the negative control reporter pRTU1 was cotransfected with different amounts of K15 or LMP1 expression constructs as indicated in the figure legends. Dominant negative mutant forms of TRAF-2, TRAF-6, Ras, Raf, and Erk2 or the respective empty expression vectors were cotransfected as indicated in the figures. After transfection, cells were maintained in medium containing 1% FCS to downregulate serum-activated signaling pathways. Cells were lysed 24 h posttransfection in reporter lysis buffer, and luciferase activity was assayed as mentioned above.

Flotation gradients. One day prior to transfection, Cos7 cells were plated in 75-cm^2 tissue culture flasks (Costar) and transfected the following day at ~50% confluency with Effectene (3.1 μg of DNA per 75-cm^2 flask) in accordance with the manufacturer's (Qiagen) instructions. At 48 h posttransfection, cells were washed once with PBS, trypsinized, resuspended in PBS, centrifuged, washed with 10 ml of PBS, counted, and pelleted. The cell pellets were resuspended in the respective volumes of ice-cold TNE buffer (10 mM Tris-HCl [pH 7.4], 150 mM NaCl, 5 mM EDTA plus protease inhibitors) containing 1% Triton X-100 to adjust the cell concentration to 10^7 cells/ml for all samples. Cells were lysed for 30 min on ice, homogenized with a 200-μl pipette (10 strokes), and centrifuged for 10 min at 900 × *g* at 4°C. One milliliter of the supernatant was mixed with 1 ml of 85% sucrose in TNE and pipetted onto the bottom of an ultracentrifuge tube (14 by 95 mm; Beckman). Six milliliters of a 35% sucrose solution in TNE was layered on top, followed by 3.5 ml of a 5% sucrose solution in TNE. The samples were subjected to ultracentrifugation at 200,000 × *g* in an SW40 rotor for 22 h at 4°C, and 1-ml fractions were collected starting at the top of the gradient. The pellet was resuspended in 200 μl of TNE containing 1% Triton X-100. Equal amounts of fractions 1 to 12 (20 μl) were analyzed by SDS-PAGE and Western blotting (of the pellet fraction, only 4 μl was loaded). Fractions 4 and 5 contain lipid rafts and the proteins associated with them. Fractions 9 to 12 contain soluble and solubilized proteins of the nonraft membrane.

RESULTS

Proteins encoded by the K15 gene and localization in lipid rafts. The KSHV K15 gene encodes several membrane proteins with a varying number of transmembrane regions and a common cytoplasmic domain (Fig. 1) (17, 34, 64). The longest

of the K15-encoded proteins, containing all eight exons, is predicted to give rise to a membrane protein of 489 aa with up to 12 transmembrane domains. When the K15 gene was transiently expressed in Cos7, HEK 293, or HEK 293-T cells, a protein of ~45 kDa was detected by immunoblotting with a polyclonal antiserum raised against the cytoplasmic domain of K15 (Fig. 2A and data not shown). Similar results were obtained with two independently constructed expression vectors for the eight-exon K15 cDNA (see Materials and Methods) which were used throughout this study. In addition, we (34) and others (17) have recently described several splice variants of K15. The K15 splice variants examined in this study are shown in Fig. 1. Whereas K15 ex1/6-8 uses exons 1, 6, 7, and 8, the splice variants K15 ex1 as/6-8 and K15 ex1 as/4-8 use an alternative splice (as) in exon 1 together with exons 6, 7, and 8 or exons 4 to 8, respectively. This implies the use of a different reading frame in exon 1. These three splice variants are predicted to encode proteins with two to four transmembrane domains. When transiently expressed in Cos7 cells, proteins of approximately 33 to 35 kDa (K15 ex1/6-8), 34 and 21 kDa (K15 ex1 as/4-8), and 26 and 21 kDa (K15 ex1 as/6-8) were detected by immunoblotting with K15 polyclonal antiserum (Fig. 2B, C, and D). The 33- to 35-kDa protein seen with K15 ex1/6-8 corresponds to the size expected for this cDNA (Fig. 2B), as do the 34- and 26-kDa proteins seen with K15 ex1 as/4-8 and K15 ex1 as/6-8, respectively (Fig. 2C and D). The additional 21-kDa protein seen with K15 ex1 as/4-8 and K15 ex1 as/6-8 (Fig. 2C and D) may be the result of alternative splicing, proteolytic processing, or internal initiation of translation. As predicted, the different K15 protein isoforms examined appeared to be membrane proteins, since subcellular fractionation experiments (data not shown) indicated that all K15 protein isoforms can be pelleted with cellular membranes after high-speed centrifugation (100,000 × *g*) of cellular extracts from which other organelles (e.g., nuclei, mitochondria) have been depleted by centrifugation at 1,000 × *g*. In addition, all K15 isoforms are located in lipid rafts, as shown by flotation experiments (Fig. 2).

Lipid rafts are membrane microdomains rich in cholesterol and sphingolipids that are resistant to solubilization with certain nonionic detergents like Triton X-100 at 4°C. Hence, lipid rafts and proteins associated with them float up to a position of lower density (5 to 35%) in a sucrose gradient in the presence of 1% Triton X-100, whereas soluble proteins and solubilized membrane proteins remain at the bottom of the gradient at the higher sucrose concentration (35 to 42.5%). As shown in Fig. 2A (top), the 45-kDa protein derived from the eight-exon K15 cDNA expression construct (K15 ex1-8; aa 1 to 489) could be detected in fractions 4 and 5 of the sucrose gradient, which represent the interface of 5 and 35% sucrose. These fractions correspond to the position of lipid rafts, as indicated by the presence of caveolin 1 (Fig. 2A, bottom). Caveolin 1 is a component of caveolae, which represent a specialized subset of lipid rafts (31, 75). K15 proteins of 33 to 35 kDa (splice variant K15 ex1/6-8 in Fig. 2B) and 21 kDa (splice variants K15 ex1 as/4-8 in Fig. 2C and K15 ex1 as/6-8 in Fig. 2D) also floated to the same position in the sucrose gradient.

Only a portion of the K15 proteins was incorporated into lipid rafts (Fig. 2). On the basis of densitometry scanning of the blots shown in Fig. 2, we estimate that 21% of the 45-kDa immunoreactive K15 protein (K15 ex1-8) (excluding the material in the pellet fraction) was present in lipid rafts. For the smaller 33- to 35-kDa K15 ex1/6-8 splice variant, a comparable amount (26%) was found in lipid rafts, in contrast to only 5% in the case of K15 ex1 as/4-8 and a similar small proportion in the case of K15 ex1 as/6-8. It thus appears that the K15 ex1

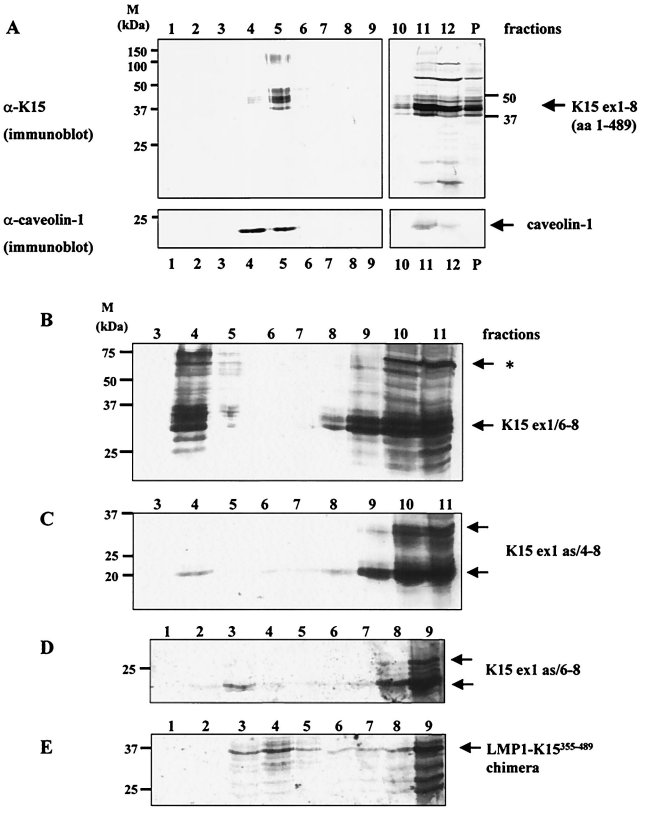

FIG. 2. The 45-kDa K15 protein (aa 1 to 489) is associated with lipid rafts. Cos7 cells were transiently transfected with K15 expression construct K15 ex1-8 (A); the natural splice variant K15 ex1/6-8 (B), K15 ex1 as/4-8 (C), or K15 ex1 as/6-8 (D); or the LMP1–K15$^{355\text{-}489}$ chimera (E). At 48 h after transfection, Cos7 cells were lysed in TNE buffer and extracts were analyzed on a flotation sucrose gradient as described in Materials and Methods. After ultracentrifugation, 1-ml fractions were collected starting at the top of the gradient and analyzed by Western blotting with a rabbit antibody to K15. Lipid raft-associated proteins are localized at the interface of 5 and 35% sucrose (fractions 4 and 5). Soluble proteins and solubilized membrane proteins of the nonraft plasma membrane are localized to the higher-density sucrose fractions (fractions 10 to 12, 35 to 42.5% sucrose). P, pellet. (A, top) The 45-kDa form of K15 ex1-8 (aa 1 to 489) localizes to lipid rafts (fractions 4 and 5, interface of 5 and 35% sucrose) and to the fractions containing solubilized membrane proteins (fractions 10 to 12, 35 to 42.5% sucrose). (A, bottom) Western blotting of the samples from the upper part of this panel probed with anti-caveolin 1. Endogenous caveolin 1 served as a positive control for lipid raft localization. (B) The 33- to 35-kDa protein derived from splice variant K15 ex1/6-8 is localized in the lipid raft fraction and high-density sucrose fractions (fractions 8 to 11). *, possible dimeric form. (C) The ~21-kDa protein derived from splice variant K15 ex1 as/4-8 (see text) is found in lipid rafts and high-density sucrose fractions. (D) The ~21-kDa protein derived from K15 ex1 as/6-8 is localized in lipid rafts and also in fractions containing solubilized membrane proteins (see text). (E) The LMP1–K15$^{355\text{-}489}$ chimera is found in lipid rafts and high-density sucrose fractions.

as/4-8 and K15 ex1 as/6-8 proteins were incorporated less efficiently than the 45-kDa (K15 ex1-8) and 33- to 35-kDa (K15 ex1/6-8) isoforms.

The eight-exon 45-kDa K15 protein (K15 ex1-8; aa 1 to 489) was also detected in fractions 10, 11, and 12 (sucrose concentrations of 35 to 42.5%) of the sucrose gradient, where solubilized membrane proteins would be expected (Fig. 2A, top). This result is reminiscent of LMP1 and LMP2A, which are both localized to lipid rafts and also to nonraft cell membranes (35). The 45-kDa K15 protein could also be detected in the pellet fraction containing cytoskeleton-associated proteins (Fig. 2A, top), which was also observed for the LMP1 protein but not for LMP2A by Higuchi et al. (35). A chimeric LMP1/K15 protein, containing the six LMP1 transmembrane domains fused to the cytoplasmic region of K15, was also found in lipid rafts and nonraft cell membranes (Fig. 2E).

K15 protein binds to and is phosphorylated by members of the Src kinase family. Since K15 resembles the LMP2A protein of EBV with respect to its genomic localization at the right end of the genome, its protein structure with 12 putative transmembrane domains, the presence of putative binding sites for SH2 and SH3 motifs in the cytoplasmic domain (17, 34), and its localization in lipid rafts, we examined whether K15 has functional characteristics in common with LMP2A. It has previously been shown that K15 is constitutively phosphorylated on the tyrosine within the distal putative SH2-binding motif Y^{481}EEVL (17). Since LMP2A is phosphorylated at its ITAM by members of the nonreceptor protein tyrosine kinase (PTK) family, we investigated whether K15 is a substrate for these kinases. The complete cytoplasmic C-terminal domain of K15 fused to GST (GST–$K15^{355-489}$) and the deletion mutant form GST–$K15^{355-472}$ lacking the distal SH2-binding motif (Y^{481}EEVL) were expressed in *E. coli* and purified as described in Materials and Methods. The purified fusion proteins were analyzed by SDS-PAGE (data not shown), and equal amounts of protein were used as the substrate in an in vitro kinase assay with immunoprecipitated myc-tagged PTKs Src, Fyn, Lck, Hck, and Yes from transiently transfected HEK 293-T cells. Figure 3A shows that all of the kinases examined phosphorylated the C-terminal domain of K15 (GST–$K15^{355-489}$, Fig. 3A, top, upper part), whereas the GST–$K15^{355-472}$ fusion protein lacking the Y^{481}EEVL motif was not phosphorylated (Fig. 3A, bottom, upper part), nor was unfused GST protein (Fig. 3A). Expression of the myc-tagged PTKs was examined with an anti-c-myc antibody (Fig. 3A).

Since the sequence deleted in the mutant form GST–$K15^{355-472}$ contains two threonine residues (T^{474} and T^{478}) that could be targets for phosphorylation by other cellular kinases, we probed the Western blots of the kinase assay reaction mixtures with an anti-phosphotyrosine antibody (Fig. 3B). The result shows that GST–$K15^{355-489}$, but not GST–$K15^{355-472}$, was phosphorylated on tyrosine, indicating that Y^{481} in the YEEVL SH2-binding motif was phosphorylated by the PTKs examined.

To investigate the binding of the C-terminal K15 domain to PTKs, we used a GST pulldown approach. GST–$K15^{355-489}$ protein expressed in *E. coli* was used to bind the myc-tagged PTKs Src, Hck, Fyn, Lck, and Yes from transiently transfected HEK 293-T cells. GST alone served as a negative control. As shown in a Western blot probed with anti-c-myc antibody, all of the PTKs examined could be precipitated with the GST–$K15^{355-489}$ protein

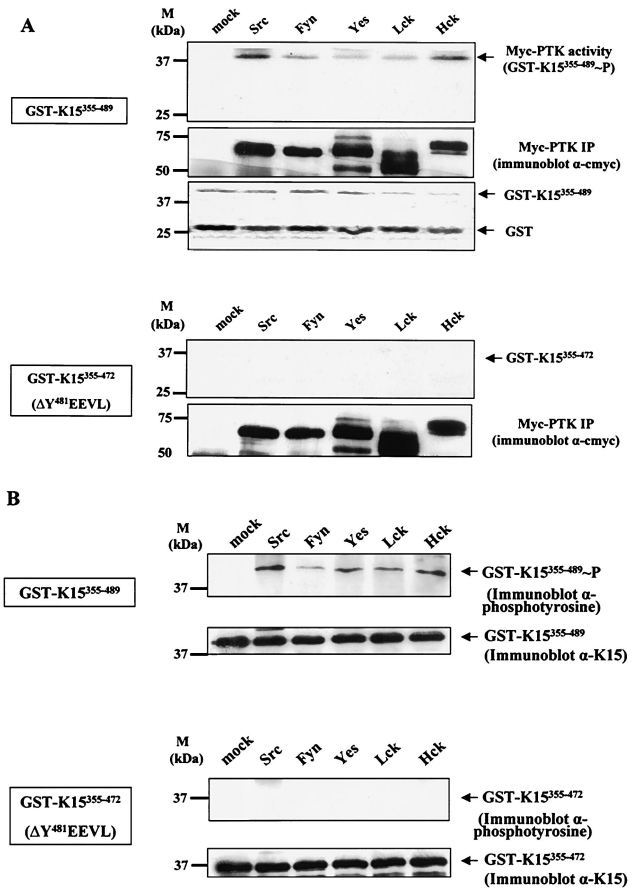

FIG. 3. The tyrosine residue of the distal SH2-binding motif (Y^{481}EEVL) of the K15 C-terminal domain is phosphorylated by members of the Src kinase family of PTKs. Purified GST–$K15^{355-489}$ and GST–$K15^{355-472}$ proteins were used as substrates in in vitro kinase assays with immunoprecipitated (IP) myc-tagged PTKs and [γ-^{32}P]ATP. (A) The PTK family members Src, Fyn, Yes, Lck, and Hck phosphorylate the C-terminal domain of K15 in an in vitro immunocomplex kinase assay (top, upper part). When the last 17 aa encompassing the SH2-binding motif (Y^{481}EEVL) of the C terminus were deleted (GST–$K15^{355-472}$), no phosphorylation was observed (bottom, upper part). The expression level of the myc-tagged immunoprecipitated Src kinases was detected with an anti-c-myc antibody (top, middle part, and bottom, lower part). The amounts of GST–$K15^{355-489}$ fusion protein and nonfused GST protein used in the in vitro kinase reactions were also analyzed with a Coomassie-stained SDS gel (top, lower part). (B) The kinase reaction mixtures shown in panel A were analyzed by Western blotting with an anti-phosphotyrosine antibody. Expression of the GST-K15 fusion proteins was detected with an anti-K15 monoclonal antibody.

(Fig. 4). In order to identify the binding site of the PTKs within the K15 cytoplasmic domain, serial deletion mutant forms of GST–$K15^{355-489}$ were constructed and used in a GST pulldown experiment. As shown in Fig. 4, all of the PTKs analyzed still bound strongly to all deletion mutants lacking, respectively, the distal SH2-binding motif Y^{481}EEVL (GST–$K15^{355-472}$), the region of aa 439 to 489 (GST–$K15^{355-438}$), and the PPLP motif (aa 387 to 390) together with the YASIL motif (aa 431 to 435) (GST–$K15^{355-373}$). As described previously (34), Y^{481}EEVL, Y^{431}ASIL, and P^{387}PLP are conserved between the K15 P and M variants and could be candidates for SH3- and SH2-binding mo-

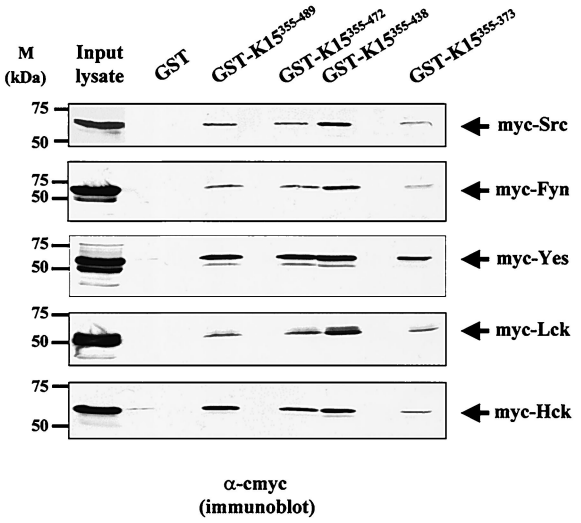

FIG. 4. The nonreceptor PTKs Src, Fyn, Yes, Lck, and Hck bind to the C-terminal domain of K15. In a GST pulldown experiment, the GST–K15$^{355-489}$, GST–K15$^{355-472}$, GST–K15$^{355-438}$, and GST–K15$^{355-373}$ fusion proteins immobilized on glutathione Sepharose beads were incubated with lysates of HEK 293-T cells transfected with expression vectors for myc-tagged PTKs. Bound PTKs were detected by Western blotting with an antibody to c-*myc*.

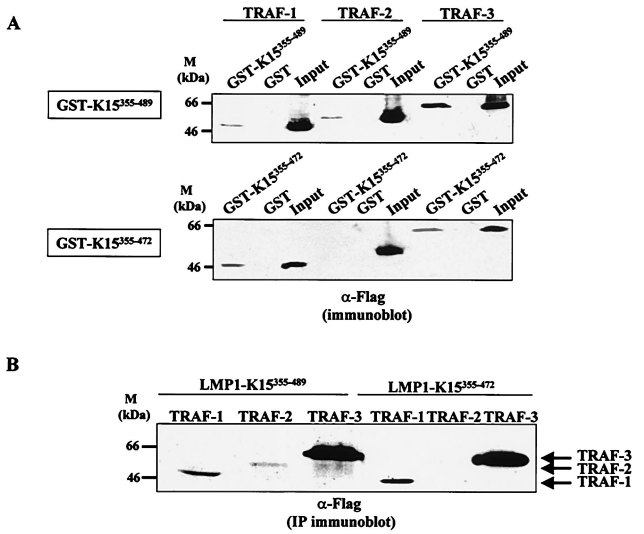

FIG. 5. Interaction of TRAF-1, -2, and -3 with the carboxy-terminal domain of K15. (A) Flag-tagged cDNA expression constructs of TRAF-1, -2, and -3 were transiently transfected into HEK 293 cells, and the interaction of the TRAF proteins with the carboxy-terminal domain of K15 (aa 355-489) was examined by GST pulldown assays as described in Materials and Methods. (Top) Interaction of TRAF with the entire carboxy-terminal domain of K15. Lanes: 1 to 3, TRAF-1-transfected cells; 4 to 6, TRAF-2-transfected cells; 7 to 9, TRAF-3-transfected cells; 1, 4, and 7, TRAF proteins bound to GST–K15$^{355-489}$; 2, 5, and 8, proteins bound to GST; 3, 6, and 9, input cell lysates. (Bottom) Interaction with the carboxy-terminal region of K15 from which the terminal 17 aa, containing the distal TRAF-like binding site, have been deleted (GST–K15$^{355-472}$). Samples were loaded as in the upper part of this panel. (B) HEK 293 cells were transiently cotransfected with Flag-tagged TRAF-1 (lanes 1 and 4), TRAF-2 (lanes 2 and 5), and TRAF-3 (lanes 3 and 6) expression constructs together with the LMP1–K15$^{355-489}$ (lanes 1 to 3) or LMP1–K15$^{355-472}$ (lanes 4 to 6) chimera. At 48 h after transfection, detergent-extracted cell lysates were immunoprecipitated (IP) with rabbit anti-K15 serum and analyzed by Western blotting, followed by staining with an anti-Flag monoclonal antibody.

tifs. Our results suggest that the most proximal region of the cytoplasmic domain of K15 contributes to the binding of Src kinases but do not exclude a role for the PPLP or YASIL motif in this interaction.

Amino acids 473 to 489 of the C terminus of K15 are required for TRAF-2 but not for TRAF-1 and -3 binding. We have previously shown that the carboxy-terminal domain of K15 (aa 355 to 489) is able to interact with TRAF-1, -2, and -3 in a GST pulldown assay (34). In order to map the binding site for TRAF-1, -2, and -3 in K15, we used GST–K15$^{355-489}$ and GST–K15$^{355-472}$ in a pulldown experiment with detergent-solubilized extracts from HEK 293 cells that had been transiently transfected with Flag-tagged cDNA constructs of TRAF-1, -2, or -3. The results confirmed our previous observation that the carboxy-terminal region of K15 interacts with TRAF-1, -2, and -3, with TRAF-3 binding more strongly than TRAF-1 and -2 (Fig. 5A, top). Deletion of aa 473 to 489 abolished the binding of TRAF-2 to K15 but not the binding of TRAF-1 and -3 (Fig. 5A, bottom). These results were further confirmed by coimmunoprecipitation experiments with the chimeric construct LMP1–K15$^{355-489}$ (Fig. 1), which was cotransfected with Flag-tagged cDNA constructs expressing TRAF-1, -2, or -3 into 293 cells (Fig. 5B). At 48 h after transfection, proteins were immunoprecipitated with the anti-K15 polyclonal serum raised against the C-terminal domain of K15 and immunoblotted with an anti-Flag monoclonal antibody. The results shown in Fig. 5B mirror those of the GST pulldown experiment, with TRAF-3 being most efficiently immunoprecipitated with the LMP1–K15$^{355-489}$ chimera, followed by TRAF-1 and -2 (Fig. 5B, lanes 1 to 3). When LMP1–K15$^{355-489}$ was replaced with the deletion mutant form LMP1–K15$^{355-472}$, binding of TRAF-2 was lost, while TRAF-1 and -3 were still efficiently precipitated (Fig. 5B, lanes 4 to 6). These results suggest a strong interaction of TRAF-1 and -3 with aa 355 to 472 and a weaker, possibly indirect, interaction of TRAF-2 with aa 472 to 489 of K15.

Activation of the NF-κB pathway by the 45-kDa K15 protein involves Y^{481}. The ability of TRAF-1, -2, and -3 to interact with K15 resembles their binding to CTAR-1 and -2 of LMP1, where they provide a link to downstream events that result in activation of the NF-κB pathway (8, 19, 20, 44, 58, 68). We investigated whether the different K15 isoforms can activate NF-κB by cotransfecting corresponding expression vectors (Fig. 1 and Materials and Methods) together with a luciferase reporter plasmid containing three NF-κB sites into HEK 293-T cells. As shown in Fig. 6, K15 ex1-8, expressing the longest K15 isoform (aa 1 to 489), showed five- to sixfold activation, whereas the smaller K15 isoforms (K15 ex1/6-8, K15 ex1 as/6-8, and K15 ex1 as/4-8) did not significantly increase basal NF-κB activity. LMP-1 induced approximately 30-fold activation of this reporter in our experiments (data not shown). In comparison, we observed only moderate (threefold) NF-κB activation with the LMP1–K15$^{355-489}$ chimeric protein (Fig. 6). Protein expression of the different constructs in HEK 293-T cells was comparable on Western blots (not shown). These results indicate a contribution of the transmembrane regions of K15 to

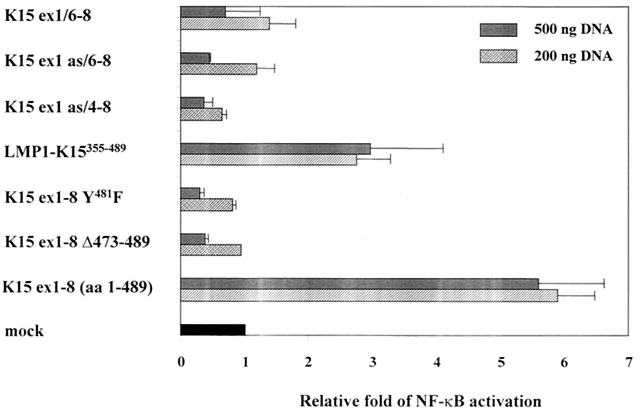

FIG. 6. The 45-kDa K15 protein activates the transcription factor NF-κB in a luciferase-based reporter assay. HEK 293-T cells were transiently cotransfected with 50 ng of the luciferase reporter plasmid p3EnhκBconA-Luc containing three NF-κB binding sites upstream of the luciferase gene and different amounts of K15 expression constructs (200 and 500 ng of DNA). At 24 h after transfection, cells were lysed and analyzed for luciferase activity. Shown is the relative fold activation compared to that of empty-vector (mock)-transfected (200 and 500 ng of DNA) cells based on triplicate samples. Equal expression levels of K15 proteins were analyzed by Western blotting with rabbit K15 antiserum (data not shown).

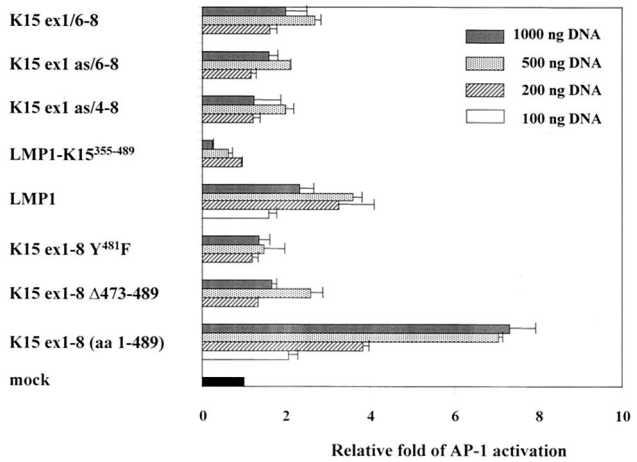

FIG. 7. Transcription factor AP-1 is activated by K15. HEK 293-T cells were transiently cotransfected with the AP-1 luciferase reporter plasmid pRTU14 containing four AP-1-binding sites upstream of the luciferase gene and different amounts of K15 expression constructs (100, 200, 500, and 1,000 ng). After transfection, cells were grown in medium containing 1% FCS, lysed after 24 h, and analyzed for luciferase activity. Shown is the relative fold activation compared to that of mock-transfected (100, 200, 500, and 1,000 ng) cells based on triplicate samples. Equal expression levels of K15 proteins were analyzed by Western blotting with rabbit K15 antiserum (data not shown).

NF-κB activation, which can also partly be provided by the LMP1 transmembrane regions. A deletion construct lacking aa 473 to 489, including the Y^{481}EEVL motif, and the K15 point mutant form of $Y^{481}\rightarrow F^{481}$ did not activate NF-κB (Fig. 6), indicating that phosphorylation of Y^{481}, most likely by members of the PTK family, is required for initiation of NF-κB signaling.

The activity of the AP-1 transcription factor is induced by K15. Mitogenic transcription factor AP-1 is a dimer of Jun-Jun or Jun-Fos family proto-oncoproteins, and it has been shown that LMP1 is an inducer of AP-1 activity in HEK 293 cells (45). To test whether K15 can activate the AP-1 transcription factor, HEK 293-T cells were transiently cotransfected with 50 ng of the reporter plasmid pRTU14, which consists of a luciferase reporter gene under the control of a minimal promoter and four AP-1-binding sites (TREs), and increasing amounts of different K15 expression constructs (Fig. 1), or plasmid pSV-LMP1 coding for the LMP1 protein as a positive control. The results depicted in Fig. 7 show that full-length K15 ex1-8 (aa 1 to 489) was a more potent inducer of AP-1 activity than was LMP1, with K15 activating AP-1 up to seven- to eightfold and LMP1 activating AP-1 up to three- to fourfold in a dose-dependent manner compared to cells transfected with control plasmids. No increase in luciferase activity was measured with the reporter control plasmid pRTU1 lacking the TREs (data not shown). AP-1 activation of the K15 deletion mutant form lacking the Y^{481}EEVL motif (K15 ex1-8 Δ473 to 489) and the point mutant form K15 ex1-8 Y^{481}F was significantly reduced. This indicates that phosphorylation of tyrosine Y^{481} of the Y^{481}EEVL motif is important for K15-induced AP-1 activation. Interestingly, the LMP1–$K15^{355-489}$ chimera did not induce AP-1 activity. The three K15 splice variants (K15 ex1/6-8, K15 ex1 as/6-8, and K15 ex1 as/4-8; Fig. 1 and 7) showed no clear-cut activation although they contain the entire K15 cytoplasmic domain. This may suggest that the regions encoded by exons 2 to 5 are also important for induction of AP-1 activity.

A K15 protein induces the kinase activity of the MAPKs Erk2 and JNK1 but not that of p38. After we had established that K15 is able to induce the AP-1 transcription factor, the next step was to elucidate the signaling pathways that mediate the signaling effects of the K15 protein. Three major MAPK pathways have been described to date that regulate AP-1 activity in the cell: the MEK1/2-Erk1/2 pathway, the MKK4/7(SEK1)-JNK1 cascade, and the MKK3/6-p38 pathway (14, 63). LMP1 induces the activity of the transcription factor AP-1 specifically via the JNK1 pathway (24, 25, 45) but does not induce the activity of the Erk2 kinase (45). Furthermore, LMP1 induces the activity of the MAPK p38 (71). In order to investigate the ability of the longest K15 isoform to induce any of these pathways, we examined the activation of the MAPKs Erk2, JNK1, and p38 in in vitro immunocomplex kinase assays. LMP1 was included in the JNK1 and p38 kinase assays as a positive control.

As depicted in Fig. 8A, the 45-kDa K15 protein (K15 ex 1-8; aa 1 to 489) was able to induce the kinase activity of cotransfected HA-tagged Erk2 kinase in transiently transfected HEK 293-T cells as measured by phosphorylation of the myelin basic protein (MBP). In contrast to the strong activation of Erk2 kinase by $K15^{1-489}$ (Fig. 8A), we only observed weak activation of JNK1 in cotransfected HEK 293-T cells (Fig. 8B). As expected, the positive control LMP1 strongly induced the kinase activity of cotransfected HA-JNK1 in HEK 293-T cells (Fig. 8B) (45). Equal amounts of HA-tagged Erk2/JNK1 being immunoprecipitated and used for the kinase assay reactions were confirmed by Western blotting with antibodies to Erk2/JNK1 protein (Fig. 8A and B, middle parts).

The activation of the Erk2 and JNK1 kinase activities in

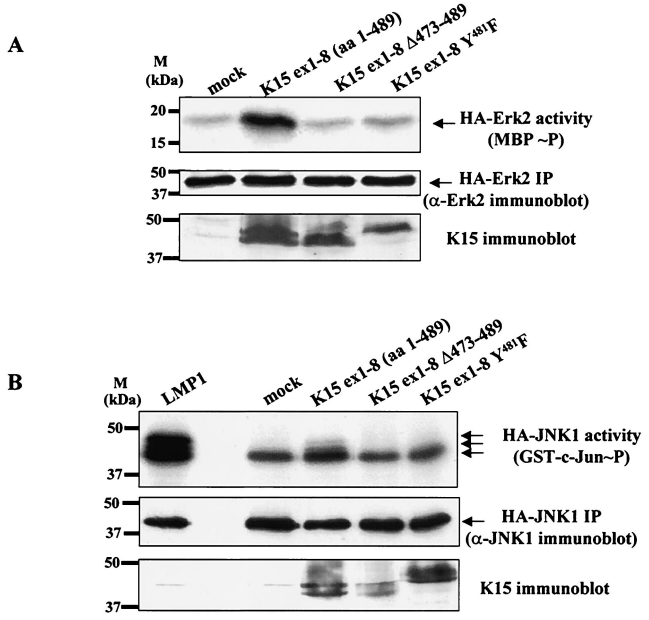

FIG. 8. Immunocomplex kinase assays with MAPKs Erk2 and JNK1. HEK 293-T cells were transiently cotransfected with 1 μg of the HA-tagged MAPK Erk2 or JNK1 and 1 μg of the K15 (Fig. 1) or LMP1 expression construct. After transfection, cells were grown in medium containing 1% FCS and lysed after 24 h in TBS-T buffer containing phosphatase inhibitors. The cell lysates were then subjected to immunoprecipitation with HA-antibody 12C5 coupled to protein G beads overnight. MBP or purified GST–c-Jun fusion protein served as the substrate in the in vitro kinase reaction mixture with Erk2 (A) or JNK1 (B), respectively. The immunoprecipitated (IP) kinase was incubated with its substrate and [γ-^{32}P]ATP for 30 min at 25°C in kinase reaction buffer and subsequently analyzed by autoradiography (top of panels A and B). Western blots of the kinase reactions were probed with specific Erk2 or JNK1 antibodies to ensure equal expression levels of the MAPKs (middle of panels A and B). Cell lysates were analyzed for equal expression of K15 constructs by Western blotting and probing with a K15 antibody (bottom of panels A and B).

HEK 293-T cells induced by the K15 protein depended on its intact cytoplasmic domain (Fig. 8A and B), since no Erk2 or JNK1 activities were observed upon cotransfection with either the deletion construct K15 ex1-8 Δ473 to 489 or the point mutant form K15 ex1-8 Y^{481}F. This suggests that phosphorylation of Y^{481}, presumably by members of the PTK family, is crucial for K15 signaling activity in these two MAPK pathways.

In similar cotransfection experiments with K15 expression vectors and HA-p38 kinase in HEK 293-T cells followed by an in vitro kinase assay with recombinant ATF-2 as the substrate, we did not observe an effect of K15 proteins on p38 kinase activity, in contrast to LMP1, which activated this pathway (data not shown; 26, 71). These findings demonstrate that the 45-kDa K15 protein specifically induced the classical MEK1/2-Erk2 MAPK pathway and, but to a lesser extent, the SEK1-JNK1 pathway but not the MKK-p38 cascade.

Dominant negative mutant forms of TRAF-2, Ras, Raf, and Erk2 and the MEK1/2-specific inhibitors PD98059 and UO126 reduce K15-induced activities of Erk2 and AP-1. Since we have demonstrated that K15 bound TRAF-2 via aa 472 to 489 of its C-terminal domain and that this region is crucial for induction of NF-κB and AP-1 activity by K15, we wanted to elucidate

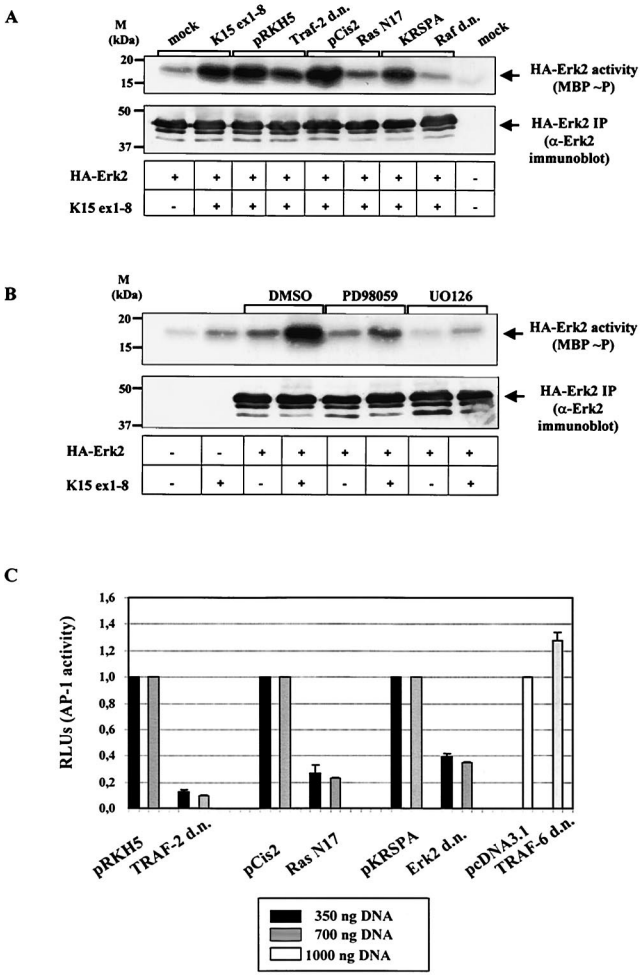

FIG. 9. Dominant negative-negative (d.n.) mutant forms of TRAF-2, Erk2, Raf, and Ras and the MEK1/2 inhibitors UO126 and PD98059 reduce the Erk2 and AP1 activation induced by K15. (A) Seven hundred nanograms of a dominant negative mutant form of TRAF-2, Ras, Raf, or Erk2 or the respective empty expression vector, pRKH5, pCis2, or pKRSPA, was cotransfected with 1 μg of HA-Erk2 and 1 μg of K15 ex1-8 (aa 1 to 489) or empty K15 expression vector (mock) where indicated. Erk2 kinase activity was monitored by phosphorylation of MBP (top). The Western blot probed with anti-Erk2 antibody shows equal expression levels of the Erk2 kinase for all samples. (B) HEK 293-T cells were cotransfected with 1 μg of HA-Erk2 and 1 μg of K15 ex1-8 (aa 1 to 489) expression construct or empty K15 expression vector. At 14 h after transfection, DMSO alone or the MEK1/2 inhibitor PD98059 or UO126 was added to the medium at 50 μM from a 50 mM stock solution in DMSO. Cells were incubated for a further 8 h before protein extraction. In vitro kinase assays were performed as described in the legend to Fig. 8 and Materials and Methods. The Western blot probed with anti-Erk2 antibody shows equal expression levels of the Erk2 kinase for all samples. (C) AP-1 luciferase-based reporter assay. HEK 293-T cells were transiently cotransfected with 50 ng of the AP-1 reporter plasmid (pRTU14), 500 ng of the K15 ex1-8 (aa 1 to 489) expression construct, and 350, 700, or 1,000 ng of a d.n. mutant form of Ras, TRAF-2, TRAF-6, or Erk2 or the respective empty expression vector, pCis2, pRKH5, pcDNA3.1, or pKRSPA. Shown are the luciferase values (in relative light units) of the different dominant negative mutant forms with respect to those of the corresponding empty expression vectors, which were set at 1.

whether a dominant negative mutant form of TRAF-2 could block K15-induced Erk2 and AP-1 activation. In order to further examine the downstream signaling routes linking K15 to Erk2, we also tested if coexpression of dominant negative mutant forms of Ras (Ras N17), Raf, or Erk2 could inhibit K15-induced Erk2 and AP-1 activation in immunocomplex kinase assays (Fig. 9A) and luciferase-based AP-1 reporter experiments (Fig. 9C). In addition, we tested the effects of two chemical MEK1/2-specific inhibitors, PD98059 (2) and UO126 (27), on the induction of Erk2 and AP-1 by K15 (Fig. 9B). MEK1/2 is the upstream kinase that phosphorylates and thereby activates Erk1/2.

Transient coexpression of dominant negative TRAF-2 with HA-Erk2 and full-length K15 reduced K15-induced Erk2 activity, as shown by decreased phosphorylation of the Erk2 substrate MBP compared to coexpression with the empty TRAF-2 vector pRKH5 in HEK 293-T cells (Fig. 9A). An even more marked inhibition by dominant negative TRAF-2 was seen in the AP-1 luciferase-based reporter assay (Fig. 9C). In order to show the specificity for TRAF-2 and since TRAF-6 is involved in LMP1-induced activation of the p38 MAPK pathway (71), we also analyzed the effect of a dominant negative TRAF-6 mutant form on K15-induced AP-1 activation. Figure 9C shows that dominant negative TRAF-6 had no effect on AP-1 induction by K15 compared to cotransfected pcDNA3.1 vector. Dominant negative Ras N17 inhibited K15-induced Erk2 and AP-1 activation, as shown in the immunocomplex kinase assay (Fig. 9A) and the reporter assay (Fig. 9C), in contrast to the empty expression vector pCis2. The dominant negative Raf mutant form reduced MBP phosphorylation by Erk2 in the immunocomplex kinase assay (Fig. 9A) but showed only moderate inhibition in the AP-1 reporter assay compared to the empty expression vector KRSPA (data not shown). In the AP-1 reporter assay, the dominant negative Erk2 mutant form (Erk C3, $Y^{185} \rightarrow F^{185}$) was able to inhibit AP-1 activation by K15, in contrast to KRSPA (Fig. 9C).

In addition to dominant negative mutant forms of the components of the Ras/Erk pathway, we also found that two chemical inhibitors of MEK1/2, PD98059 and UO126, inhibited K15-induced Erk2 activity in an immunocomplex kinase assay (Fig. 9B). Likewise, in the AP-1 reporter assay, both PD98059 and UO126 at 50 μM inhibited K15-induced AP-1 activity by approximately 50 to 60% (data not shown). These results suggest that K15 signals via the Ras/Erk pathway involving the components Ras, Raf, MEK, and Erk2 and that TRAF-2 may be involved in linking this pathway to K15 phosphorylated on Y^{481}.

DISCUSSION

We show here that the major isoform of K15-derived proteins, containing all eight exons and presumably 489 aa, activated the Ras/MAPK pathway, as well as the NF-κB pathway and, more weakly, the MAPK JNK. Activation of these pathways depended on Y^{481} in a carboxy-terminal YEEVL motif that is reminiscent of the YEEA motif surrounding Y^{112} of EBV LMP2A. In B cells, Y^{112} of LMP2A is phosphorylated by, and important for the recruitment of, the Src kinases Lyn and Fyn (30). We could show that several Src kinases, including Src, Fyn, Yes, Hck, and Lck, could phosphorylate Y^{481} of K15 in vitro (Fig. 3). However, sequences located between aa 355 and 373, at the beginning of the cytoplasmic domain of K15, appear to contribute to the interaction of Src kinases with the K15 cytoplasmic domain, since a GST-K15 fusion protein containing this region still bound to all of the Src kinases tested (Fig. 4). This observation does not exclude an additional role for the PPLP or YASIL motif in Src kinase binding. A $Y^{481}F$ mutant form abolished the ability of the major K15 protein to activate the Ras/MAPK pathway, as well as JNK and NF-κB (Fig. 6, 7, and 8), indicating that phosphorylation of Y^{481}, presumably by members of the Src kinase family, represents a first step in the activation of these pathways.

Constitutive phosphorylation of K15 Y^{481} in B cells has been reported by others (17), although the kinases involved were not identified. This group also found that a CD8-K15 chimeric protein could inhibit B-cell receptor-initiated signaling in the B-cell line BJAB but was unable to initiate Ca^{2+} mobilization after cross-linking with an antibody to CD8 (17). In our study, the nature of the transmembrane anchor appeared to be important for the ability of K15-derived proteins to initiate different signaling pathways, since only the longest isoform, containing 12 putative transmembrane domains (Fig. 1) (17, 34, 64), was capable of initiating efficient signaling (Fig. 6 and 7). Even the six transmembrane domains of LMP1, which can mediate efficient clustering of LMP1 in the cell membrane as a prerequisite for constitutive intracellular signaling (32), were unable to induce activation of an AP-1 reporter when fused to the cytoplasmic region of K15 (Fig. 1 and 7) and only showed moderate activation of an NF-κB reporter compared to the longest K15 isoform (Fig. 6). Although we did not examine Ca^{2+} mobilization as a consequence of K15-initiated signaling, we think that it is therefore possible that the CD8-K15 chimeric protein used by Choi et al. (17) may have been also unable to trigger these signaling pathways.

Lipid rafts serve as platforms in cellular membranes that can incorporate and recruit membrane-associated molecules required for the assembly of signaling cascades (reviewed in reference 75). We therefore examined whether the longest K15 isoform (which is capable of inducing intracellular signaling) differs from the smaller isoforms (which are not) with respect to their incorporation into lipid rafts. We found that at least the isoform K15 ex1/6-8, which contains the complete first exon, appeared to be incorporated into lipid rafts to roughly the same extent as the longest K15 isoform (Fig. 2A and B). In contrast, the two isoforms K15 ex1 as/6-8 and K15 ex1 as/4-8, which use an alternative splice acceptor in exon 1 and therefore contain only 6 aa derived from the first exon in a different reading frame (Fig. 1) (17, 34), may be incorporated less efficiently into lipid rafts (Fig. 2C and D). Since the LMP1-K15 chimeric protein was also incorporated into lipid rafts (Fig. 2E), it appears as if differential incorporation into lipid rafts is not responsible for the fact that these membrane proteins differ in the ability to initiate intracellular signaling. Sequences encoded by K15 exons 2 to 5 may therefore contribute to intracellular signaling by providing sites for posttranslational modification or by interacting with other intracellular components.

Is there a functional role for the smaller K15 isoforms? The study by Choi et al. (17) suggests that a signaling-inactive K15 variant could inhibit intracellular signaling pathways. It is

therefore conceivable that the smaller K15 isoforms may play a role in modulating the effect of the eight-exon isoform on the activation of the pathways reported here. This would represent a parallel to the presumed role of the LMP2 splice variant LMP2B, which is devoid of the amino-terminal intracellular domain of LMP2A, but could modify LMP2A-induced signaling by affecting the clustering of LMP2A molecules in the cell membrane. RT-PCR studies of PEL cell lines (17, 34) suggest that the transcript encoding the longest K15 isoform is more strongly expressed than those encoding the smaller isoforms. A recent report (74) attributed the presence of an approximately 23-kDa K15-derived protein in PEL cell lines to internal proteolytic processing of the approximately 45-kDa (exons 1 to 8) K15 precursor protein. We have seen proteins of a similar size in PEL cells that are, however, not associated with cellular membranes, in contrast to the approximately 21-kDa proteins translated from K15 splice variants and shown in Fig. 2 to be associated with lipid rafts (Brinkmann et al., unpublished data). Whether the balance in virus-infected cells is therefore in favor of the 45-kDa activating K15 protein or in favor of the smaller nonactivating forms is unclear and may be difficult to predict from the relative abundance of individual transcripts.

In activating the Ras/MAPK pathway, the K15 eight-exon protein resembles LMP2A, which has recently been reported to activate Erk in HEK 293 cells, thereby increasing the stability of c-jun (15), although others have not seen activation of Ras/MAPK by LMP2A in epithelial cells (70). We did not investigate whether one of the downstream effects of Ras/MAPK activation by K15 is the increased stability of c-jun but found moderately increased JNK activity following transfection of K15. It remains a possibility that this weak activation of the JNK pathway occurs indirectly, perhaps as a consequence of the activation of other pathways, such as the Ras/MAPK pathway. Our preliminary studies of cDNA arrays also indicate that the expression of c-jun may be increased at the transcriptional level following K15 transfection (data not shown). There may therefore be multiple routes for LMP2A and K15 to increase the activity of the JNK/c-jun pathway which would contribute to the increased activity of the AP-1 transcription factor following K15 expression, as reported here.

Our results also suggest an involvement of TRAF-2 in the K15-induced activation of the Ras/MAPK pathway, since a dominant negative mutant form of TRAF-2 inhibited the activity of Erk2 and AP-1 in K15-transfected cells (Fig. 9). We also observed weak binding of TRAF-2 to the cytoplasmic domain of K15, which was abolished by deletion of the last 17 aa, including the Y^{481}EEVL motif, as well as the sequence ATQPTDD, which appears to be distantly related to the TRAF-binding consensus site PxQxS/T (residues identical to those of CTAR-1 of LMP1 are underlined) (Fig. 5) (34). In contrast, the stronger interaction with TRAF-1 and -3 seems to occur through a more membrane-proximal region of K15. It is therefore conceivable that the interaction of the K15 cytoplasmic domain with TRAF-2 occurs in an indirect manner. TRAF-2 mediates the activation of the p38/MAPK pathway, as well as the activation of NF-κB induced by LMP-1, CTAR-1 and -2, and possibly JNK (24, 46). The effect of LMP1 on p38/MAPK also involves TRAF-6 downstream of TRAF-2 (71), and TRAF-6 has recently been shown to be involved in the interleukin-1-induced activation of p38/MAPK via Ras (60) and in the CD40-induced activation of Erk via a Ras-independent pathway (42). However, K15-induced AP-1 activity was not affected by cotransfection of a dominant-negative mutant form of TRAF-6 (Fig. 9C), suggesting that other intracellular factors may link the cytoplasmic domain of K15, phosphorylated on Y^{481}, to the activation of the Ras/MAPK pathway. This issue, and the identity of cellular and viral genes affected by K15-induced Ras/MAPK activation, is currently under investigation.

ACKNOWLEDGMENTS

Expression constructs of dominant negative mutant forms of Erk2 and Raf and the expression vector KRSPA were generous gifts of S. Ludwig. We thank S. Müller, M. Rothe, and A. Eliopoulos for providing PTK and TRAF expression constructs and plasmids pSG-LMP1 and p3EnhκBconA-Luc. The excellent technical assistance of H. Pommer and I. Szabados is gratefully acknowledged. Finally, we greatly appreciate helpful discussions with S. Ludwig and B. Sodeik.

This work was supported by grants from the Medical Research Council, United Kingdom (G9811424), and the Deutsche Forschungsgemeinschaft (Schu 1436-1/1).

REFERENCES

1. **Albrecht, J.-C., U. Friedrich, C. Kardinal, J. Koehn, B. Fleckenstein, S. M. Feller, and B. Biesinger.** 1999. Herpesvirus ateles gene product Tio interacts with non-receptor protein tyrosine kinases. J. Virol. **73:**4631–4639.
2. **Alessi, D. R., A. Cuenda, P. Cohen, D. T. Dudley, and A. R. Saltiel.** 1995. PD 098059 is a specific inhibitor of the activation of mitogen-activated protein kinase kinase in vitro and in vivo. J. Biol. Chem. **270:**27489–27494.
3. **Baud, V., Z. G. Liu, B. Bennett, N. Suzuki, Y. Xia, and M. Karin.** 1999. Signaling by proinflammatory cytokines: oligomerization of TRAF2 and TRAF6 is sufficient for JNK and IKK activation and target gene induction via an amino-terminal effector domain. Genes Dev. **13:**1297–1308.
4. **Biesinger, B., A. Y. Tsyganov, H. Fickenscher, F. Emmrich, B. Fleckenstein, J. B. Bolen, and B. M. Bröker.** 1995. The product of the herpesvirus saimiri open reading frame 1 (Tip) interacts with T-cell specific kinase $p56^{lck}$ in transformed cells. J. Biol. Chem. **270:**4729–4734.
5. **Blasig, C., C. Zietz, B. Haar, F. Neipel, S. Esser, N. H. Brockmeyer, E. Tschachler, S. Colombini, B. Ensoli, and M. Sturzl.** 1997. Monocytes in Kaposi's sarcoma lesions are productively infected by human herpesvirus 8. J. Virol. **71:**7963–7968.
6. **Boshoff C., T. F. Schulz, M. M. Kennedy, A. K. Graham, C. Fisher, A. Thomas, J. O. McGee, R. A. Weiss, and J. J. O'Leary.** 1995. Kaposi's sarcoma-associated herpesvirus infects endothelial and spindle cells. Nat. Med. **1:**1274–1278.
7. **Boshoff, C., S. J. Gao, L. E. Healy, S. Matthews, A. J. Thomas, L. Coignet, R. A. Warnke, J. A. Strauchen, E. Matutes, O. W. Kamel, P. S. Moore, R. A. Weiss, and Y. Chang.** 1998. Establishing a $KSHV^+$ cell line (BCP-1) from peripheral blood and characterizing its growth in Nod/SCID mice. Blood **91:**1671–1679.
8. **Brodeur, S. R., G. Cheng, D. Baltimore, and D. A. Thorley-Lawson.** 1997. Localization of the major NF-κB-activating site and the sole TRAF3 binding site of LMP-1 defines two distinct signaling motifs. J. Biol. Chem. **272:**19777–19784.
9. **Bruder, J. T., G. Heidecker, and U. R. Rapp.** 1992. Serum-, TPA-, and Ras-induced expression from Ap-1/Ets-driven promoters requires Raf-1 kinase. Genes Dev. **6:**545–556.
10. **Caldwell, R. G., J. B. Wilson, S. J. Anderson, and R. Longnecker.** 1998. Epstein-Barr virus LMP2A drives B-cell development and survival in the absence of normal B-cell receptor signals. Immunity **9:**405–411.
11. **Caldwell, R. G., R. C. Brown, and R. Longnecker.** 2000. Epstein-Barr virus LMP2A-induced B-cell survival in two unique classes of EμLMP2A transgenic mice. J. Virol. **74:**1101–1113.
12. **Cesarman, E., Y. Chang, P. S. Moore, J. W. Said, and D. M. Knowles.** 1995. Kaposi's sarcoma-associated herpesvirus-like DNA sequences in AIDS-related body-cavity-based lymphomas. N. Engl. J. Med. **332:**1186–1191.
13. **Chang, Y., E. Cesarman, M. S. Pessin, F. Lee, J. Culpepper, D. M. Knowles, and P. S. Moore.** 1994. Identification of herpesvirus-like DNA sequences in AIDS-associated Kaposi's sarcoma. Science **266:**1865–1869.
14. **Chang, L., and M. Karin.** 2001. Mammalian MAP kinase signalling cascades. Nature **410:**37–40.
15. **Chen, S.-Y., J. Lu, Y.-C. Shih, and C.-H. Tsai.** 2002. Epstein-Barr virus latent membrane 2A regulates c-Jun protein through extracellular signal-regulated kinase. J. Virol. **76:**9556–9561.
16. **Chiou, C.-J., L. J. Poole, P. S. Kim, D. M. Ciufo, J. S. Cannon, C. M. ap Rhys, D. J. Alcendor, J.-C. Zong, R. F. Ambinder, and G. S. Hayward.** 2002.

Patterns of gene expression and a transactivation function exhibited by the vGCR (ORF74) chemokine receptor protein of Kaposi's sarcoma-associated herpesvirus. J. Virol. **76:**3421–3439.
17. **Choi, J.-K., B.-S. Lee, S. N. Shim, M. Li, and J. U. Jung.** 2000. Identification of the novel K15 gene at the rightmost end of the Kaposi's sarcoma-associated herpesvirus genome. J. Virol. **74:**436–446.
18. **Damania, B., J.-K. Choi, and J. U. Jung.** 2000. Signaling activities of gammaherpesvirus membrane proteins. J. Virol. **74:**1593–1601.
19. **Devergne, O., E. Hatzivassiliou, K. M. Izumi, K. M. Kaye, M. F. Kleijnen, E. Kieff, and G. Mosialos.** 1996. Association of TRAF1, TRAF2, and TRAF3 with an Epstein-Barr virus LMP1 domain important for B-lymphocyte transformation: role in NF-κB activation. Mol. Cell. Biol. **16:**7098–7108.
20. **Devergne, O., E. Cahir McFarland, G. Mosialos, K. M. Izumi, C. F. Ware, and E. Kieff.** 1998. Role of the TRAF binding site and NF-κB activation in Epstein-Barr virus latent membrane protein 1-induced cell gene expression. J. Virol. **72:**7900–7908.
21. **Duboise, S. M., J. Guo, S. Czajak, R. C. Desrosiers, and J. U. Jung.** 1998. STP and Tip are essential for herpesvirus saimiri oncogenicity. J. Virol. **72:**1308–1313.
22. **Dupin, N., C. Fisher, P. Kellam, S. Ariad, M. Tulliez, N. Franck, E. van Marck, D. Salmon, I. Gorin, J. P. Escande, R. A. Weiss, K. Alitalo, and C. Boshoff.** 1999. Distribution of human herpesvirus-8 latently infected cells in Kaposi's sarcoma, multicentric Castleman's disease, and primary effusion lymphoma. Proc. Natl. Acad. Sci. USA **96:**4546–4551.
23. **Eliopoulos, A. G., M. Stack, C. W. Dawson, K. M. Kaye, L. Hodgkin, S. Sihota, M. Rowe, and L. S. Young.** 1997. Epstein-Barr virus-encoded LMP1 and CD40 mediate IL-6 production in epithelial cells via an NF-κB pathway involving TNF receptor-associated factors. Oncogene **14:**2899–2916.
24. **Eliopoulos, A. G., and L. S. Young.** 1998. Activation of the cJun N-terminal kinase (JNK) pathway by the Epstein-Barr virus-encoded latent membrane protein 1 (LMP1). Oncogene **16:**1731–1742.
25. **Eliopoulos, A. G., S. M. Blake, J. E. Floettmann, M. Rowe, and L. S. Young.** 1999. Epstein-Barr virus-encoded latent membrane protein 1 activates the JNK pathway through its extreme C terminus via a mechanism involving TRADD and TRAF2. J. Virol. **73:**1023–1035.
26. **Eliopoulos, A. G., N. J. Gallagher, S. M. Blake, C. W. Dawson, and L. S. Young.** 1999. Activation of the p38 mitogen-activated protein kinase pathway by Epstein-Barr virus-encoded latent membrane protein 1 coregulates interleukin-6 and interleukin-8 production. J. Biol. Chem. **274:**16085–16096.
27. **Favata, M. F., K. Y. Horiuchi, E. J. Manos, A. J. Daulerio, D. A. Stradley, W. S. Feeser, D. E. Van Dyk, W. J. Pitts, R. A. Earl, F. Hobbs, R. A. Copeland, R. L. Magolda, P. A. Scherle, and J. M. Trzaskos.** 1998. Identification of a novel inhibitor of mitogen-activated protein kinase kinase. J. Biol. Chem. **273:**18623–18632.
28. **Flory, E., A. Hoffmeyer, U. Smola, U. R. Rapp, and J. T. Bruder.** 1996. Raf-1 kinase targets GA-binding protein in transcriptional regulation of the human immunodeficiency virus type 1 promoter. J. Virol. **70:**2260–2268.
29. **Fruehling, S., and R. Longnecker.** 1997. The immunoreceptor tyrosine-based activation motif of Epstein-Barr virus LMP2A is essential for blocking BCR-mediated signal transduction. Virology **235:**241–251.
30. **Fruehling, S., R. Swart, K. M. Dolwick, E. Kremmer, and R. Longnecker.** 1998. Tyrosine 112 of latent membrane protein 2a is essential for protein tyrosine kinase loading and regulation of Epstein-Barr virus latency. J. Virol. **72:**7796–7806.
31. **Galbiati, F., B. Razani, and M. P. Lisanti.** 2001. Emerging themes in lipid rafts and caveolae. Cell **106:**403–411.
32. **Gires, O., U. Zimber-Strobl, R. Gonella, M. Ueffing, G. Marschall, R. Zeidler, D. Pich, and W. Hammerschmidt.** 1997. Latent membrane protein 1 of Epstein-Barr virus mimics a constitutively active receptor molecule. EMBO J. **16:**6131–6140.
33. **Gires, O., F. Kohlhuber, E. Kilger, M. Baumann, A. Kieser, C. Kaiser, R. Zeidler, B. Scheffer, M. Ueffing, and W. Hammerschmidt.** 1999. Latent membrane protein 1 of Epstein-Barr virus interacts with JAK3 and activates STAT proteins. EMBO J. **11:**3064–3073.
34. **Glenn, M., L. Rainbow, F. Aurade, A. Davison, and T. F. Schulz.** 1999. Identification of a spliced gene from Kaposi's sarcoma-associated herpesvirus encoding a protein with similarities to latent membrane proteins 1 and 2A of Epstein-Barr virus. J. Virol. **73:**6953–6963.
35. **Higuchi, M., K. Izumi, and E. Kieff.** 2001. Epstein-Barr virus latent-infection membrane proteins are palmitoylated and raft-associated: protein 1 binds to the cytoskeleton through TNF receptor cytoplasmic factors. Proc. Natl. Acad. Sci. USA **98:**4675–4680.
36. **Hsu, H., H. B. Shu, M. G. Pan, and D. V. Goeddel.** 1996. TRADD-TRAF2 and TRADD-FADD interactions define two distinct TNF receptor 1 signal transduction pathways. Cell **84:**299–308.
37. **Huen, D. S., S. A. Henderson, D. Croom-Carter, and M. Rowe.** 1995. The Epstein-Barr virus latent membrane protein-1 (LMP1) mediates activation of NF-κB and cell surface phenotype via two effector regions in its carboxy-terminal cytoplasmic domain. Oncogene **10:**549–560.
38. **Ikeda, M., A. Ikeda, L. C. Longan, and R. Longnecker.** 2000. The Epstein-Barr virus latent membrane protein 2A PY motif recruits WW domain-containing ubiquitin-protein ligases. Virology **268:**178–191.
39. **Ikeda, M., A. Ikeda, and R. Longnecker.** 2001. PY motifs of Epstein-Barr virus LMP2A regulate protein stability and phosphorylation of LMP2A-associated proteins. J. Virol. **75:**5711–5718.
40. **Izumi, K. M., and E. Kieff.** 1997. The Epstein-Barr virus oncogene product latent membrane protein 1 engages the tumor necrosis factor receptor-associated death domain protein to mediate B lymphocyte growth transformation and activate NF-κB. Proc. Natl. Acad. Sci. USA **94:**12592–12597.
41. **Jung, J. U., S. M. Lang, T. Jun, T. M. Roberts, A. Veillette, and R. C. Desrosiers.** 1995. Downregulation of Lck-mediated signal transduction by tip of herpesvirus saimiri. J. Virol. **69:**7814–7822.
42. **Kashiwada, M., Y. Shirakata, J.-I. Inoue, H. Nakano, K. Okazaki, K. Okumura, T. Yamamoto, H. Nagaoka, and T. Takemori.** 1998. Tumor necrosis factor receptor-associated factor 6 (TRAF6) stimulates extracellular signal-regulated kinase (ERK) activity in CD40 signaling along a Ras-independent pathway. J. Exp. Med. **187:**237–244.
43. **Katano, H., Y. Sato, T. Kurata, S. Mori, and T. Sata.** 2000. Expression and localization of human herpesvirus 8-encoded proteins in primary effusion lymphoma, Kaposi's sarcoma, and multicentric Castleman's disease. Virology **269:**335–344.
44. **Kaye, K. M., O. Devergne, J. N. Harada, K. M. Izumi, R. Yalamanchili, E. Kieff, and G. Mosialos.** 1996. Tumor necrosis factor receptor associated factor 2 is a mediator of NF-κB activation by latent infection membrane protein 1, the Epstein-Barr virus transforming protein. Proc. Natl. Acad. Sci. USA **93:**11085–11090.
45. **Kieser, A., E. Kilger, O. Gires, M. Ueffing, W. Kolch, and W. Hammerschmidt.** 1997. Epstein-Barr virus latent membrane protein-1 triggers AP-1 activity via the c-Jun N-terminal kinase cascade. EMBO J. **16:**6478–6485.
46. **Kieser, A., C. Kaiser, and W. Hammerschmidt.** 1999. LMP1 signal transduction differs substantially from TNF receptor 1 signaling in the molecular functions of TRADD and TRAF2. EMBO J. **18:**2511–2521.
47. **Lam, N., and B. Sugden.** 2003. CD40 and its viral mimic, LMP1: similar means to different ends. Cell Signal. **15:**9–16.
48. **Lee, H., R. Veazey, K. Williams, M. Li, J. Guo, F. Neipel, B. Fleckenstein, A. Lackner, R. C. Desrosiers, and J. U. Jung.** 1998. Deregulation of cell growth by the K1 gene of Kaposi's sarcoma-associated herpesvirus. Nat. Med. **4:**435–440.
49. **Lee, H., J. Guo, M. Li, J. K. Choi, M. deMaria, M. Rosenzweig, and J. U. Jung.** 1998. Identification of an immunoreceptor tyrosine-based activation motif of K1 transforming protein of Kaposi's sarcoma-associated herpesvirus. Mol. Cell. Biol. **18:**5219–5228.
50. **Longnecker, R., and C. L. Miller.** 1996. Regulation of Epstein-Barr virus latency by latent membrane protein 2. Trends Microbiol. **4:**38–42.
51. **Longnecker, R.** 2000. Epstein-Barr virus latency: LMP2, a regulator or means for Epstein-Barr virus persistence? Adv. Cancer Res. **79:**175–200.
52. **Ludwig, S., K. Engel, A. Hoffmeyer, G. Sithanandam, B. Neufeld, D. Palm, M. Gaestel, and U. R. Rapp.** 1996. 3pK, a novel mitogen-activated protein (MAP) kinase-activated protein kinase, is targeted by three MAP kinase pathways. Mol. Cell. Biol. **16:**6687–6697.
53. **Merchant, M., R. G. Caldwell, and R. Longnecker.** 2000. The LMP2A ITAM is essential for providing B cells with development and survival signals in vivo. J. Virol. **74:**9115–9124.
54. **Miller, C. L., A. L. Burkhardt, J. H. Lee, B. Stealey, R. Longnecker, J. B. Bolen, and E. Kieff.** 1995. Integral membrane protein 2 of Epstein-Barr virus regulates reactivation from latency through dominant negative effects on protein-tyrosine kinases. Immunity **2:**155–166.
55. **Minden, A., A. Lin, T. Smeal, B. Derijard, M. Cobb, R. Davis, and M. Karin.** 1994. c-Jun N-terminal phosphorylation correlates with activation of the JNK subgroup but not the ERK subgroup of mitogen-activated protein kinases. Mol. Cell. Biol. **14:**6683–6688.
56. **Mitchell, T., and B. Sugden.** 1995. Stimulation of NF-κB-mediated transcription by mutant derivatives of the latent membrane protein of Epstein-Barr virus. J. Virol. **69:**2968–2976.
57. **Moore, P. S., and Y. Chang.** 1998. Kaposi's sarcoma-associated herpesvirus encoded oncogenes and oncogenesis. J. Natl. Cancer Inst. Monogr. **23:**65–71.
58. **Mosialos, G., M. Birkenbach, R. Yalamanchili, T. VanArsdale, C. Ware, and E. Kieff.** 1995. The Epstein-Barr virus transforming protein LMP1 engages signaling proteins for the tumor necrosis factor receptor family. Cell **80:**389–399.
59. **Natoli, G., A. Costanzo, A. Ianni, D. J. Templeton, J. R. Woodgett, C. Balsano, and M. Levrero.** 1997. Activation of SAPK/JNK by TNF receptor 1 through a noncytotoxic TRAF2-dependent pathway. Science **275:**200–203.
60. **Palsson McDermott, E. P., and L. A. J. O'Neill.** 2002. Ras participates in the activation of p38 MAPK by interleukin-1 by associating with IRAK, IRAK2, TRAF6, and TAK-1. J. Biol. Chem. **277:**7808–7815.
61. **Panousis, C. G., and D. T. Rowe.** 1997. Epstein-Barr virus latent membrane protein 2 associates with and is a substrate for mitogen-activated protein kinase. J. Virol. **71:**4752–4760.
62. **Parravicini, C., B. Chandran, M. Corbellino, E. Berti, M. Paulli, P. S. Moore, and Y. Chang.** 2000. Differential viral protein expression in Kaposi's sarcoma-associated herpesvirus-infected diseases: Kaposi's sarcoma, primary effusion lymphoma, and multicentric Castleman's disease. Am. J. Pathol. **156:**743–749.

63. **Pearson, G., F. Robinson, T. Gibson, B. Xu, M. Karandikar, K. Berman, and M. Cobb.** 2001. Mitogen-activated protein (MAP) kinase pathways: regulation and physiological functions. Endocr. Rev. **22:**153–183.
64. **Poole, L. J., J.-C. Zong, D. M. Ciufo, D. J. Alcendor, J. S. Cannon, R. Armbinder, J. M. Orenstein, M. S. Reitz, and G. S. Hayward.** 1999. Comparison of genetic variability at multiple loci across the genomes of the major subtypes of Kaposi's sarcoma-associated herpesvirus reveals evidence for recombination and for two distinct types of open reading frame K15 alleles at the right-hand end. J. Virol. **73:**6646–6660.
65. **Rainbow, L., G. M. Platt, G. R. Simpson, R. Sarid, S.-J. Gao, H. Stoiber, C. S. Herrington, P. S. Moore, and T. F. Schulz.** 1997. The 222- to 234-kilodalton latent nuclear protein (LNA) of Kaposi's sarcoma-associated herpesvirus (human herpesvirus 8) is encoded by orf73 and is a component of the latency-associated nuclear antigen. J. Virol. **71:**5915–5921.
66. **Rickinson, A., and E. Kieff.** 2001. Epstein-Barr virus, p. 2573–2627. *In* D. M. Knipe, P. M. Howley, D. E. Griffin, R. A. Lamb, M. A. Martin, B. Roizman, and S. E. Straus (ed.), Virology, 4th ed. Lippincott Williams & Wilkins, Philadelphia, Pa.
67. **Robbins, D. J., E. Zhen, H. Owaki, C. A. Vanderbilt, D. Ebert, T. D. Geppert, and M. H. Cobb.** 1993. Regulation and properties of extracellular signal-regulated protein kinases 1 and 2 in vitro. J. Biol. Chem. **268:**5097–5106.
68. **Sandberg, M., W. Hammerschmidt, and B. Sugden.** 1997. Characterization of LMP-1's association with TRAF1, TRAF2, and TRAF3. J. Virol. **71:**4649–4656.
69. **Scholle, F., R. Longnecker, and N. Raab-Traub.** 1999. Epithelial cell adhesion to extracellular matrix proteins induces tyrosine phosphorylation of the Epstein-Barr virus latent membrane protein 2: a role for C-terminal Src kinase. J. Virol. **73:**4767–4775.
70. **Scholle, F., K. M. Bendt, and N. Raab-Traub.** 2000. Epstein-Barr virus LMP2A transforms epithelial cells, inhibits cell differentiation, and activates Akt. J. Virol. **74:**10681–10689.
71. **Schultheiss, U., S. Püschner, E. Kremmer, T. W. Mak, H. Engelmann, W. Hammerschmidt, and A. Kieser.** 2001. TRAF6 is a critical mediator of signal transduction by the viral oncogene latent membrane protein 1. EMBO J. **20:**5678–5691.
72. **Schulz, T. F.** 1999. Epidemiology of Kaposi's sarcoma-associated herpesvirus (KSHV/HHV8). Adv. Cancer Res. **76:**121–160.
73. **Schulz, T. F.** 2001. KSHV/HHV8-associated lymphoproliferations in the AIDS setting. Eur. J. Cancer **37:**1217–1226.
74. **Sharp, T. V., H.-W. Wang, A. Koumi, D. Hollyman, Y. Endo, H. Ye, M.-Q. Du, and C. Boshoff.** 2002. K15 protein of Kaposi's sarcoma-associated herpesvirus is latently expressed and binds to HAX-1, a protein with antiapoptotic function. J. Virol. **76:**802–816.
75. **Simons, K., and D. Toomre.** 2000. Lipid rafts and signal transduction. Nat. Rev. **1:**31–41.
76. **Soulier, J., L. Grollet, E. Oksenhendler, P. Cacoub, D. Cazals-Hatem, P. Babinet, M. F. d'Agay, J. P. Clauvel, M. Raphael, and L. Degos.** 1995. Kaposi's sarcoma-associated herpesvirus-like DNA sequences in multicentric Castleman's disease. Blood **86:**1276–1280.
77. **Troppmair, J., J. T. Bruder, H. Munoz, P. A. Lloyd, J. Kyriakis, P. Banerjee, J. Avruch, and U. R. Rapp.** 1994. Mitogen-activated protein kinase/extracellular signal-regulated protein kinase activation by oncogenes, serum, and 12-*O*-tetradecanoylphorbol-13-acetate requires Raf and is necessary for transformation. J. Biol. Chem. **269:**7030–7035.
78. **Winberg, G., L. Matskova, F. Chen, P. Plant, D. Rotin, G. Gish, R. Ingham, I. Ernberg, and T. Pawson.** 2000. Latent membrane protein 2A of Epstein-Barr virus binds WW domain E3 protein-ubiquitin ligases that ubiquitinate B-cell tyrosine kinases. Mol. Cell. Biol. **20:**8526–8535.